



Toward untangling thunderstorm-aerosol relationships: An observational study of regions centered on Washington, DC and Kansas City, MO

Mace Bentley ^{a,*}, Tobias Gerken ^a, Zhuojun Duan ^b, Dudley Bonsal ^a, Henry Way ^a, Endre Szakal ^b, Mia Pham ^b, Hunter Donaldson ^a, Lucie Griffith ^a

^a School of Integrated Sciences, James Madison University, Harrisonburg, VA, USA

^b Department of Computer Science, James Madison University, Harrisonburg, VA, USA

ARTICLE INFO

Keywords:

Lightning
Thunderstorm
Aerosols
Thermodynamics

ABSTRACT

A multi-variable investigation of thunderstorm environments in two distinct geographic regions is conducted to assess the aerosol and thermodynamic environments surrounding thunderstorm initiation. 12-years of cloud-to-ground (CG) lightning flash data are used to reconstruct thunderstorms occurring in a 225 km radius centered on the Washington, D.C. and Kansas City Metropolitan Regions. A total of 196,836 and 310,209 thunderstorms were identified for Washington, D.C. and Kansas City, MO, respectively. Hourly meteorological and aerosol data were then merged with the thunderstorm event database.

Evidence suggests, warm season thunderstorm environments in benign synoptic conditions are considerably different in thermodynamics, aerosol properties, and aerosol concentrations within the Washington, D.C. and Kansas City regions. However, thunderstorm intensity, as measured by flash counts, appears regulated by similar thermodynamic-aerosol relationships despite the differences in their ambient environments. When examining thunderstorm initiation environments, there exists statistically significant, positive relationships between convective available potential energy (CAPE) and flash counts. Aerosol concentration also appears to be a more important quantity than particle size for lightning augmentation.

1. Introduction and background

Land cover and the thermodynamic properties of the atmospheric boundary layer modify thunderstorms and their signature phenomena, lightning. Some of the sharpest contrasts in thunderstorms on the globe occur along the continental-ocean boundary (Williams and Stanfill, 2002). In general, the land has an order-of-magnitude greater amount of lightning than the ocean (Christian, 2003). Thermodynamic properties of the atmosphere change greatly because of differences in surface land cover. There are also accompanying changes in the size and concentration of particulate matter that also account for differences in lightning activity (Wall et al., 2014; Fuchs et al., 2015; Li et al., 2017). Although isolating thermodynamic, wind, and aerosol mechanisms may be useful in terms of simplifying a description of causality, it overlooks interactions arising out of their mutual embeddedness (Williams et al., 2002; 2004; Carrió and Cotton, 2011).

Aerosolized particulate matter includes species that can be activated as cloud condensation nuclei (CCN) and significantly modify the

organization of cloud systems across multiple scales (van den Heever and Cotton, 2007; Fan et al., 2008; Wang et al., 2011). For example, Huang et al. (2022) found a positive correlation ($R \sim 0.6-0.7$) of surface PM10 and cloud base aerosols. CCN activation is dependent on physiochemical properties such as particle size (i.e. PM10; PM25), chemical components, and the mixing state of the atmosphere (Wu et al., 2013; Zhang et al., 2017; Wang et al., 2023a, 2023b). The amount of naturally and anthropogenically sourced aerosols within the mixing layer substantially alter cloud microphysics and influence the cloud growth process, warm rain production, precipitation rates, and cloud electrification (Rosenfeld and Lensky, 1998; Konwar et al., 2012; Rosenfeld et al., 2014, 2016, 2019; Zhu et al., 2014, 2015; Guo et al., 2018; Huang et al., 2022).

The multi-scaled interactions of thermodynamic and aerosol processes that promote atmospheric convection have been recognized as critically important for understanding climate change (Fan et al., 2013; Li et al., 2017). Broad, satellite-data driven comparisons of land-ocean and urban-rural convective activity recognize the importance of

* Corresponding author.

E-mail address: bentleml@jmu.edu (M. Bentley).

interactions between thermodynamic and aerosol mechanisms (Khain et al., 2008; Fan et al., 2009; Stallins et al., 2013; Lopez, 2016; Stolz et al., 2017). While the physical basis for thermodynamic and aerosol feedbacks has been established, the spatial and temporal expression of their embeddedness at urban and regional scales remains poorly understood (Sun et al., 2023).

Moisture, temperature, and lapse rates are important variables used to predict the likelihood of thunderstorms (Craven and Brooks, 2004; Williams et al., 2005; Wang et al., 2009). Measurements for these parameters at different pressure levels are commonly used to evaluate stability, like convective available potential energy (CAPE; Emanuel, 1994; Blanchard, 1998; Zipser, 2003; Bang and Zipser, 2016). However, thunderstorm convection and lightning production also involve aerosol processes (Andreae, 2004; Khain et al., 2005, 2008; van den Heever et al., 2006, 2011; Tao et al., 2007, 2012; Rosenfeld et al., 2008, 2014; Altaratz et al., 2014; Li et al., 2017; Wang et al., 2023a, 2023b). When boundary-layer air contains more aerosols, cloud droplets are often more numerous but smaller in diameter. As a result, there is more upward transport of water above the freezing level. A mixture of graupel, snow crystals, and supercooled water droplets create conditions for charge separation and lightning production (Reynolds et al., 1957). At temperatures less than -15°C , graupel and snow crystals become negatively and positively charged, respectively. Different particle sizes and fall velocities generate further charge separation. The negatively charged graupel accumulates in the middle of the cloud while the positively charged snow crystals are more numerous in the upper cloud. At temperatures above approximately -15°C , the polarities can reverse (Reynolds et al., 1957).

Vertical motion is also enhanced in polluted air because of extra latent heat release caused by prolonged condensational droplet growth and additional freezing (Khain et al., 2005; Rosenfeld et al., 2008; Carrión et al., 2010; Li et al., 2017; Sun et al., 2023). Lower aerosol concentrations have the opposite effect, diminishing lightning due to cloud water being shared among a smaller number of cloud droplets and condensation nuclei (Sun et al., 2023). With early rainout and less vertical transport into the mixed phase region, there is significantly less thunderstorm charging (Rosenfeld et al., 2008). Evidence suggests that the convective activity promoting lightning may increase up to a threshold amount, and then decline as higher aerosol concentrations act to diminish insulation and stabilize the atmosphere (Rosenfeld et al., 2002; van den Heever and Cotton, 2007; Rosenfeld et al., 2008; Fuchs et al., 2015). Higher concentrations of aerosols can warm the surrounding atmospheric layer, reduce the relative humidity, and cool the surface. This stabilizes temperature profiles below the aerosol layer, leading to a reduction in lightning activity and the noted “boomerang effect” (Koren et al., 2008; Altaratz et al., 2010; Li et al., 2017).

These threshold processes have been dubbed the cloud lifetime effect (Stevens and Feingold, 2009) since aerosols shape not only the intensity of convection and lightning production, but also its duration. A corollary of these dynamics is that a given quantity of atmospheric instability can have differing amounts of lightning production depending on aerosol concentrations. Conversely, more CAPE may be required to increase lightning production under higher aerosol loads. While modeling has provided the mechanistic details of these interactions across simulated boundary conditions (van den Heever et al., 2006; Ekman et al., 2011; Fan et al., 2013; Schmid and Niyogi, 2017; Sun et al., 2023), there are a lack of observational investigations that examine this variability within the constraints of measured atmospheric conditions and thunderstorm lifecycles.

Using cloud-to-ground (CG) lightning as an indicator of thunderstorm strength, we characterize the response to aerosol and thermodynamic environments surrounding two distinct urban areas in the United States: Washington, DC and Kansas City, MO. This investigation represents an emerging focus in synoptic climatology and meteorology: the scale at which aerosols and thermodynamic mechanisms interact to shape processes relevant to high impact weather. Evidence suggests that

day-to-day weather phenomena like thunderstorms are responding to complex aerosol feedback mechanisms operating at the mesoscale (Rosenfeld et al., 2008; Bell et al., 2009; Koren et al., 2010, 2012; Storer et al., 2014; Fuchs et al., 2015; Igel and van den Heever, 2015; Li et al., 2017; Wang et al., 2023a, 2023b). Variability in tropospheric aerosols occurs at horizontal scales of 40–400 km and temporal scales of 2–48 h (Anderson et al., 2003). Such variation is below the traditional synoptic or airmass scale, where aerosol properties are often assumed to be homogeneous (Sheridan, 2002). However, cities, where aerosol regimes are highly changeable, can also generate considerable variability in how local atmospheres modify thunderstorms (Petersen and Rutledge, 2001; Shepherd, 2005; Wang et al., 2011; Ashley et al., 2012; Stallins et al., 2013; Coquillat et al., 2013; Schmid and Niyogi, 2017; Kingfield et al., 2018; Wang et al., 2023a, 2023b). By examining the spatiality of urban thunderstorm variability and its relationship with aerosols and thermodynamics, we conduct a multi-variable investigation of thunderstorm environments in two distinct geographic regions (Fig. 1). Data mining techniques are employed to examine how variation of thermodynamic instability, aerosols, and lightning frequencies covary across two distinct geographic regions. This analysis investigates interactions between thermodynamics and aerosols on thunderstorm development and thus avoids a binary framework that focuses on either alone.

2. Data and methodology

2.1. Study region

By comparing thermodynamic-aerosol-thunderstorm relationships among two distinct urban regions, we can draw more inferences about their interrelationships. Regional weather patterns vary in their propensity for producing thunderstorms and lightning. However, these weather patterns can also be associated with different transport directions and concentrations of air pollution (Power, 2003; Keim et al., 2005; Power et al., 2006; Sheridan et al., 2008; Diem et al., 2010; Fuchs et al., 2015). Although aerosols may correlate with meteorological conditions, by comparing two locations, one can logically delineate some of these relationships. Across the two urban areas selected for this study, one would encounter more permutations of weather type, aerosol regime, and land cover. This would provide a larger “state space” for examining a range of aerosol and thermodynamic conditions and how they are expressed in the geographic patterns of thunderstorm occurrence.

The Washington, DC metropolitan area, which includes parts of Maryland, Virginia, and West Virginia, is the country’s sixth-largest metropolitan area with a 2020 population of 6.3 million, and over 54 million people residing within 400 km of the city (Fig. 1a). The city is in the mid-Atlantic region, along the U.S. East Coast. The metropolitan area is 16,882 km², with a population density of 378 people per km² (US Census Bureau, 2021). Washington, DC is in a maritime region within the humid subtropical climate zone (Köppen: Cfa). Summers are hot and humid with a July daily average of 26.6 °C and average daily relative humidity around 66%. Heat indices regularly approach 38 °C. The combination of heat and humidity in the summer also brings convective instability that produced frequent thunderstorms and lightning activity.

Kansas City, Missouri is the largest city in Missouri by population and area (Fig. 1b). The Kansas City metropolitan area includes urban areas across the Kansas-Missouri state borders, with Kansas City, Missouri as the largest city. The Kansas City metropolitan area has a population of 2.2 million people, with an area of 18,796 km², and a population density of 117 people per km² (US Census Bureau, 2021). The Kansas and Missouri rivers cut wide valleys into the terrain and a partially filled spillway valley crosses the central city. Although Kansas City contains some areas of steeper relief, the highest and lowest points in Kansas City are only 313 and 220 m above sea level, respectively. The city is in a continental region and lies in the northern periphery of the humid subtropical zone. The warmest month is July, with an average

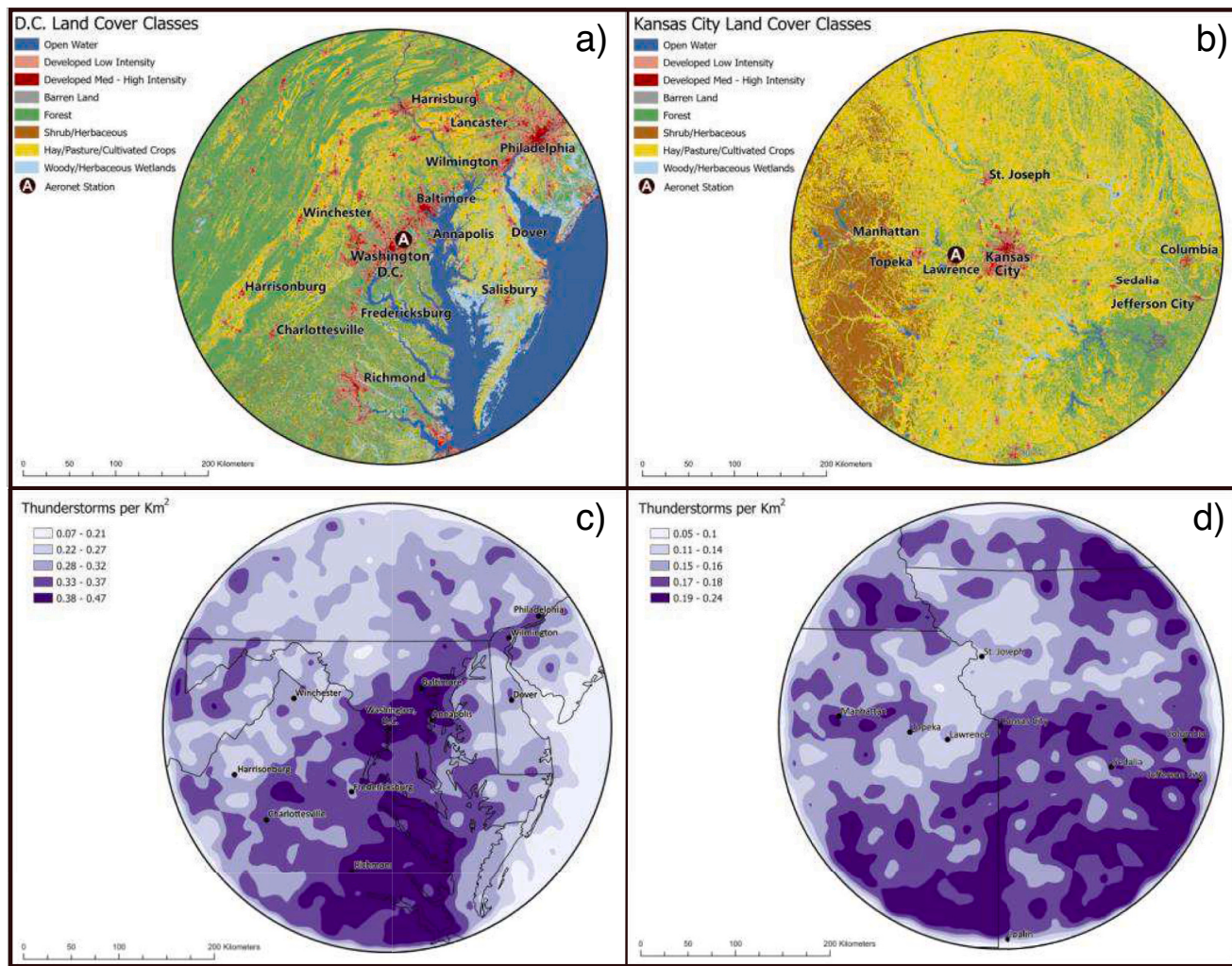


Fig. 1. a) Washington, DC study area. b) Kansas City, MO study area. c) same as a), except for the kernel density of the initiation locations of 74,328 thunderstorms with >10 flashes. d) same as b), except for the kernel density of the initiation locations of 33,732 thunderstorms with >10 flashes occurring between noon and 8 pm. Land cover for 2021 obtained from the USGS National Land Cover Database.

temperature of 27.2 °C. The summer months are hot and humid, with high temperatures surpassing 32 °C on 47 days.

2.2. Thunderstorm event database

This investigation utilizes National Lightning Detection Network (NLDN) cloud-to-ground (CG) lightning data for a 12-year period (2006–2010; 2013–2015; 2017–2020) within a 225-km radius centered on the Washington, DC and Kansas City Metropolitan Regions (Vaisala, Inc.; Fig. 1). The years 2011, 2012, and 2016 were excluded from the analysis due to missing data. To concentrate on thunderstorms developing in weakly-forced synoptic environments, where thermodynamic-aerosol-thunderstorm relationships would be more discernible, the Spatial Synoptic Classification scheme (v3.0) was utilized to identify days with transitional weather typologies (Sheridan, 2002). Transitional weather days are defined as days where the weather typology changes and exhibits large shifts in pressure, dew point, and wind (Sheridan, 2002). Evidence suggests that thunderstorms most susceptible to urban effects occur during non-transitional weather days (Dixon and Mote, 2003; Bentley et al., 2010). Therefore, flashes occurring on days with a transitional or missing synoptic classification were removed from the investigation. Approximately 32% of all flashes in Washington, DC and 45% of all flashes for Kansas City, occurred on transitional weather days. Additionally, only flashes recorded during the warm season, defined by

those months capturing at least 90% of the annual lightning and encompassing May through September, were used in the analyses. NLDN CG lightning detection efficiencies for the study period are 90–95% and locational accuracies are <500 m. Upgrades in the NLDN necessitate that we also remove positive CG lightning flashes <15 kA (Cummins et al., 1998; Rudlosky and Fuelberg, 2010).

A thunderstorm-tracking algorithm based on Tuomi and Larjavaara (2005) was developed that identifies thunderstorms by their lightning characteristics. Individual thunderstorms produce a path of CG lightning as they propagate and evolve; therefore, the identification of thunderstorms by lightning generation is possible. Prior research in thunderstorm event detection using lightning data provided a methodology useful to parse the 7,207,567 flashes and 14,796,725 flashes in our study regions surrounding Washington, DC and Kansas City, MO, respectively (Tuomi and Larjavaara, 2005; Rose et al., 2008). Lightning flashes in the dataset were grouped into individual thunderstorms by means of the following temporal and spatial clustering algorithm (Fig. 2; modified from Tuomi and Larjavaara, 2005):

1. The NLDN dataset was initially placed into time sequential order.
2. Each flash was input from the NLDN dataset and tested with respect to existing thunderstorms using the following conditions:

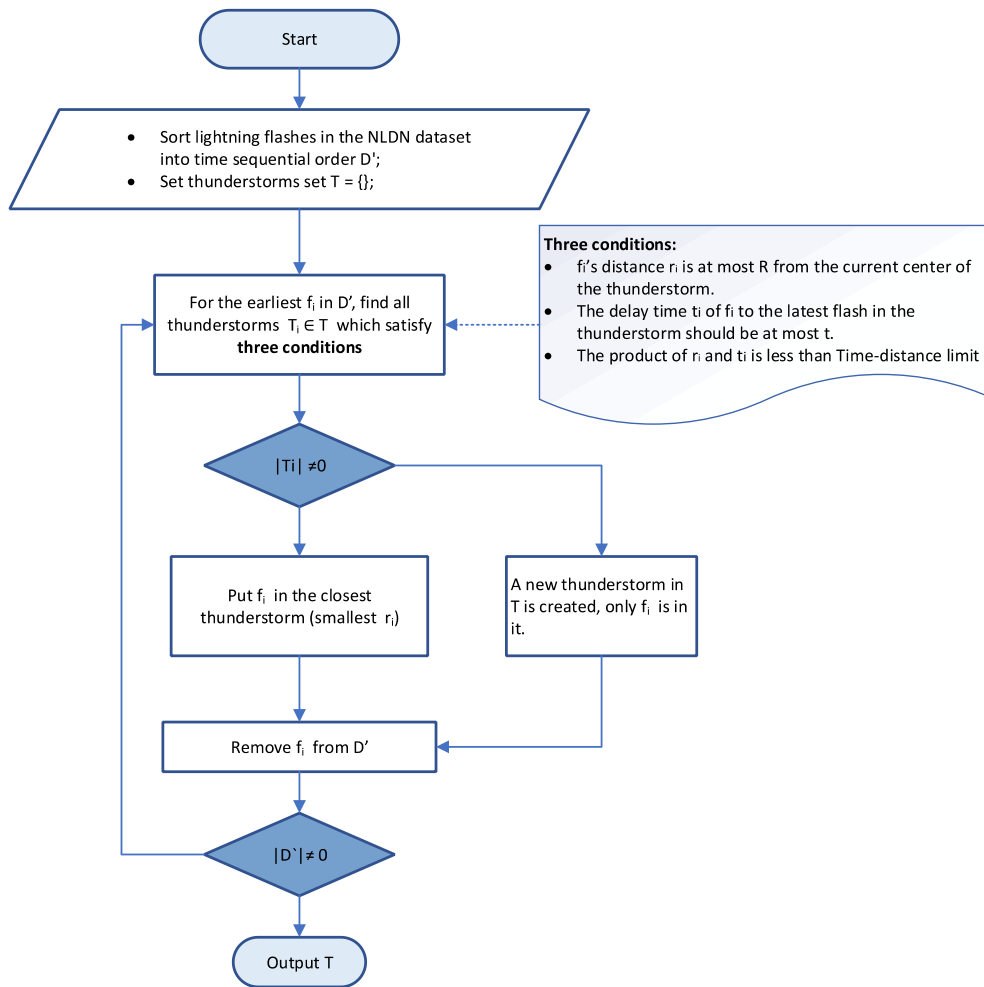


Fig. 2. Flow diagram of the temporal and spatial clustering algorithm.

a) Radius of attraction, R. A new flash may be accepted to a thunderstorm if its distance is, at most, R from the current center of the thunderstorm. Evidence suggests that R = 15 km provides an optimum spacing distance between flashes within a thunderstorm (Tuomi and Larjavaara, 2005; Rose et al., 2008). The center of a thunderstorm is approximated by the average location of recently occurring flashes. Recently occurring flashes are defined by the location of the most recent 20 flashes, or less in a newly forming thunderstorm.

b) Delay time, t. The delay time from the newest flash to the latest flash in the thunderstorm should be, at most, t. Evidence suggests t = 15 min provides an optimum temporal spacing between subsequent flashes and those within a thunderstorm (Tuomi and Larjavaara, 2005; Rose et al., 2008). All flashes exceeding this temporal limit are not considered for inclusion, in which case the thunderstorm is closed and not tested further for future flash inclusion.

c) Time-distance limit. Since conditions a) and b) together are not always sufficient to prevent a relatively distant flash from being joined to a thunderstorm and forming a bridge to an adjacent storm, the time-distance of the new flash from the latest flash in the thunderstorm is also evaluated. If the product of the time and distance exceeds a defined threshold, the flash is not accepted into the thunderstorm. The time-distance limit can be used to fine-tune the algorithm. Lower time-distance limits lead to the identification of thunderstorms with smaller total flash counts and less bridging of adjacent storms. Higher time-distance limits produce thunderstorms with larger total flash counts and can bridge adjacent storms into a

single thunderstorm event. After testing different time-distance limits to assess sensitivity, a time-distance limit = 10 was chosen to most accurately identify individual thunderstorms and limit the potential of bridging adjacent storms.

d) Closest thunderstorm. If more than one thunderstorm fulfills conditions a), b), and c), the closest storm (smallest R) is chosen for the lightning flash (Tuomi and Larjavaara, 2005).

e) New thunderstorm. If no thunderstorm is found in d), the new flash begins a new thunderstorm.

Hourly meteorological, aerosol, and ECMWF ERA5 gridded data were then added into the thunderstorm event database by identifying the time and location of the first flash (defined as the thunderstorm initiation) in each thunderstorm and incorporating the closest measurement (in time and distance) from the atmospheric, aerosol, pollution, and gridded datasets.

Hourly, level 2.0 AERONET data from the NASA Goddard Space Flight Center, Greenbelt, MD and Lawrence, Kansas sites were used to obtain the spectral, 500 nm aerosol optical depth (AOD, a dimensionless measure of particle concentration) and 675–440 nm Angstrom exponent (AE, a dimensionless measure related to particle size distribution) in the vertical column (Fig. 1). AERONET Level 2.0 data have been thoroughly screened for cloud contamination and are correlated with satellite-based estimates of AOD (Green et al., 2009; Li et al., 2009). The AOD–Angstrom exponent scatter plot is a common tool used to classify aerosol types. Morales Rodriguez et al. (2010) used AERONET data as part of a characterization of thunderstorm versus non-thunderstorm

days.

We also incorporated the U.S. Environmental Protection Agency's (EPA) hourly measurements of particulate matter with diameters that are generally 10 μm and smaller (PM10) and particulate matter with diameters that are generally 2.5 μm and smaller (PM2.5) as correlates of aerosol concentration. These data were collected from 272 and 179 air quality stations within the Washington, DC and Kansas City regions, respectively. The nearest station corresponding to the thunderstorm event initiation in space and time was chosen for the PM10 and PM2.5 measurement. If >3 h elapsed between the thunderstorm initiation time and the closest PM10 or PM2.5 measurement, it was denoted as missing. The mean distance from the thunderstorm initiation locations to the closest PM10 and PM2.5 measurements were 35 km for both measurements in the Kansas City region, and 18 km and 20 km, respectively for both measurements in the Washington, DC region. PM10 and PM2.5 have been found useful as measures for aerosols in lightning investigations when accounting for surface air temperature and CAPE (Li et al., 2018). Although PM concentration measurements at the surface are not necessarily representative of the particle distribution available in the atmospheric column for the development of clouds, near-time, proximal pollution measurements for thunderstorm initiation environments throughout the day have been found useful in evaluating aerosol impacts on convection (Stallins et al., 2013; Pérez-Invernón et al., 2021; Yair et al., 2022).

The ECMWF ERA5 hourly, 30-km gridded dataset was used to estimate CAPE for the initiation location of each thunderstorm. The CAPE is calculated hourly for each grid point by considering parcels of air departing at different model levels below 350 hPa. ERA5 is produced using 4D-Var data assimilation and model forecasts in CY41R2 of the ECMWF Integrated Forecast System (IFS), with atmospheric data interpolated to 37 pressure levels (Hersbach et al., 2020).

The thunderstorm event databases constructed for the Washington, DC and Kansas City regions include the corresponding aerosol and meteorological variables closest in time and space for each thunderstorm's initiation and dissipation (defined as the time and location of the last flash). Additional information includes each thunderstorm's total flash count and a unique ID that links thunderstorms to their associated flashes.

2.3. Statistical analysis

Covariation between CAPE and aerosol quantities (AOD, PM10, and PM2.5) were analyzed by assigning data to four percentile-based bins using 50th, 75th and 90th percentiles as bin edges. This approach ensures an adequate number of events for statistical analysis in all bins, while also allowing for analysis of the impacts of more extreme thermodynamic and aerosol conditions. We are not examining the impact of PM 2.5 and PM10 on CAPE, but rather examine the relationship of thunderstorm flash counts, a measure of thunderstorm strength, as a function of their covariance.

Before calculating percentiles, physically unrealistic negative values were eliminated from the dataset. While analyzing the probability density distribution of AOD values for Kansas City, we noticed an excessive occurrence of observations with a single value (AOD = 0.048) within the dataset and we proceeded to eliminate AOD values of <0.05 from the analysis.

We report the bin average for all quantities as well as their confidence intervals (5th - 95th percentile). Confidence intervals were generated using $n = 1000$ bootstrapped samples (James et al., 2013).

3. Results and discussion

Our analysis grouped the lightning flashes into a total of 196,836 thunderstorm events in the Washington DC region, while 310,209 thunderstorms were identified from the flash database for Kansas City. Over 37.7% and 39.2% of all thunderstorm events consisted of >10

flashes for Washington, DC and Kansas City, respectively (Fig. 1c and d). Times used in the analyses and discussion are local (EDT for Washington, DC and CDT for Kansas City).

3.1. Study limitations

Several limitations exist in this investigation due to the utilization of observational datasets. While the NLDN is one of the most validated and referenced lightning detection networks in the world with over 1000 scientific references, it is calibrated to detect cloud-to-ground flashes. Given the 12-year span of this study examining two different locations, it was important to utilize a stable, quality-controlled lightning database across the temporal and spatial domains. Therefore, given that the investigation utilizes the NLDN dataset, only cloud-to-ground flashes are used in developing the thunderstorm database and in examining relationships between variables. The thunderstorm initiation environment is defined as the time and location of the first cloud-to-ground lightning flash of the thunderstorm. Initial storm electrification likely begins before the first cloud-to-ground flash; however, the applied thunderstorm event definition yields a stable, consistent criteria for identification of thunderstorm initiation employing the NLDN. As total lightning identification instruments and databases continue to be optimized, developed, and extend into longer time frames, future investigations may wish to incorporate these data into similar analyses. Total lightning activity may prove more sensitive to relationships between lightning, aerosols, thermodynamics, and to the complete cloud electrification life cycle.

Additionally, given the importance of the aerosol data in relation to storm position when evaluating relationships, the spatial density and hourly measurements from the air quality stations and AERONET networks may lack the precision to detail the in-cloud environments of the ice-phase microphysics during the lifecycle of thunderstorms. Therefore, increasing the sample size of thunderstorm events from both cities across a large range of aerosol and thermodynamic environments, aims to refine the analysis's accuracy through examining interrelationships of aerosols and thermodynamics. Through assessing urban thunderstorm variability, testing its relationship with aerosols and thermodynamics, and using the results to understand the role of urban areas in augmenting thunderstorm activity, our goal is to advance the understanding of urban weather environments and their associated thunderstorms.

3.2. Temporal thunderstorm distribution

In the Washington, DC region, the annual distribution of thunderstorms producing at least 10 flashes during the 12-year period varies from a minimum of 3946 events in 2017 to a maximum of 8220 in 2008. In the Kansas City region, the variation ranges from 8166 in 2007 to 18,903 in 2019. The Kansas City region recorded 205% more flashes and 158% more thunderstorms than Washington, DC. Outside of Florida and portions of the Gulf Coast, eastern Kansas has some of the highest flash densities in the contiguous U.S. The Washington, DC region records considerably lower flash counts, consistent with previous studies (Orville and Huffines, 2001).

For the warm season, the month with the most thunderstorms is July for Washington, DC with 21,334 events, and June for Kansas City with 31,381 events. Both study regions have September as the month with the least thunderstorms – 5299 for Washington, DC and 11,905 for Kansas City.

The distribution of thunderstorm events by day of the week illustrates an interesting pattern (Table 1). Both regions exhibit the highest frequency of thunderstorm occurrence on Thursday, with Monday and Friday being the day of the week with the fewest thunderstorm occurrences for Washington, DC and Kansas City, respectively (Table 1). The Thursday peak and Monday minimum in thunderstorm occurrence is similar to the lightning day distribution in the Tel-Aviv Metropolitan Area (Yair et al., 2022). The Washington, DC region exhibits

Table 1

Thunderstorms with at least 10 flashes as well as their relative distribution (%), by day of the week.

Weekday	Washington D.C		Kansas City, MO	
	All Events	Afternoon (12:00-8 pm)	All Events	Afternoon (12:00-8 pm)
	Number (%)	Number (%)	Number (%)	Number (%)
Monday	9073 (12.2)	5639 (12.2)	17,846 (14.7)	5518 (16.2)
Tuesday	10,787 (14.5)	6761 (14.6)	17,241 (14.2)	5153 (15.2)
Wednesday	12,205 (16.4)	7552 (16.3)	17,566 (14.4)	4679 (13.8)
Thursday	13,116 (17.6)	8415 (18.2)	17,982 (14.8)	5549 (16.3)
Friday	9783 (13.2)	6427 (13.9)	16,173 (13.3)	3973 (11.7)
Saturday	9693 (13.0)	5423 (11.7)	17,298 (14.2)	4780 (14.1)
Sunday	9671 (13.0)	6121 (13.2)	17,649 (14.5)	4347 (12.8)

considerable day-of-the-week variance with respect to thunderstorm occurrence, with Monday having only 69% of the thunderstorms occurring on Thursday (Table 1). When examining thunderstorm events occurring between 12 pm and 8 pm, the Kansas City region exhibits slightly less day-of-the-week variance, with Friday having approximately 71% of the thunderstorms occurring on Thursday.

The Washington, DC region also appears to illustrate a similar pattern to Atlanta, GA in terms of thunderstorm occurrence by day of the week (Stallins et al., 2013; Table 1). Saturday, Sunday, and Monday were minima in lightning flashes for the Atlanta area, like minima in thunderstorm occurrence in Washington, DC. Likewise, Thursday, Wednesday, and Tuesday recorded higher flash counts in Atlanta,

similar to thunderstorm occurrence in Washington, DC (Table 1; Stallins et al., 2013). Aerosol variability by weekday versus weekend was significantly correlated to the daily flash variance identified in Atlanta, GA (Stallins et al., 2013).

Considerable differences exist between the hourly distribution of thunderstorm flash counts of Washington, DC and Kansas City. Washington, DC warm season thunderstorm flash counts follow a diurnal heating curve with the peak hour of flash counts occurring at 4 pm EDT (Fig. 3a). Minima in thunderstorm flash counts occurs at 10 am, before daytime heating and convective instability significantly increase in typical humid, subtropical environments. The Kansas City region exhibits a two-peak distribution in thunderstorm flash counts (Fig. 3b). There exists an early evening secondary peak in thunderstorm flash counts (7 pm CDT), likely produced by diurnal heating; however, the early morning peak at 4 am is more persistent and lasts several hours from midnight onwards (Fig. 3). Evidence suggests that this thunderstorm activity is due to mesoscale convective system formation and the development of a nocturnal low-level jet, a common occurrence in the Great Plains (Banta et al., 2002). Nocturnal low-level jet development produces the low-level convergence and advection of unstable air necessary to support large thunderstorm complexes during the overnight hours in the warm season (Cotton and Anthes, 1989; Augustine and Caracena, 1994; Stensrud, 1996; Zhong et al., 1996; Higgins et al., 1997; Arritt et al., 1997; Tuttle and Davis, 2006; Wang and Chen, 2009).

When removing the impact of nocturnal thunderstorms, Kansas City exhibits a similar peak and lower weekend distribution in thunderstorm occurrence to Washington, DC and Atlanta, GA (12:00-8 pm; Table 1). Thursday remains the peak day of thunderstorm occurrence with secondary maxima occurring on Monday and Tuesday. A minimum of thunderstorms occurred on Friday, with only 71% of thunderstorms occurring when compared to Thursday (Table 1). This weekly variance in weekday versus weekend events suggests that the differences in day-of-the-week thunderstorm occurrence in Washington, DC and during the afternoon in the Kansas City region are possibly tied to variability in

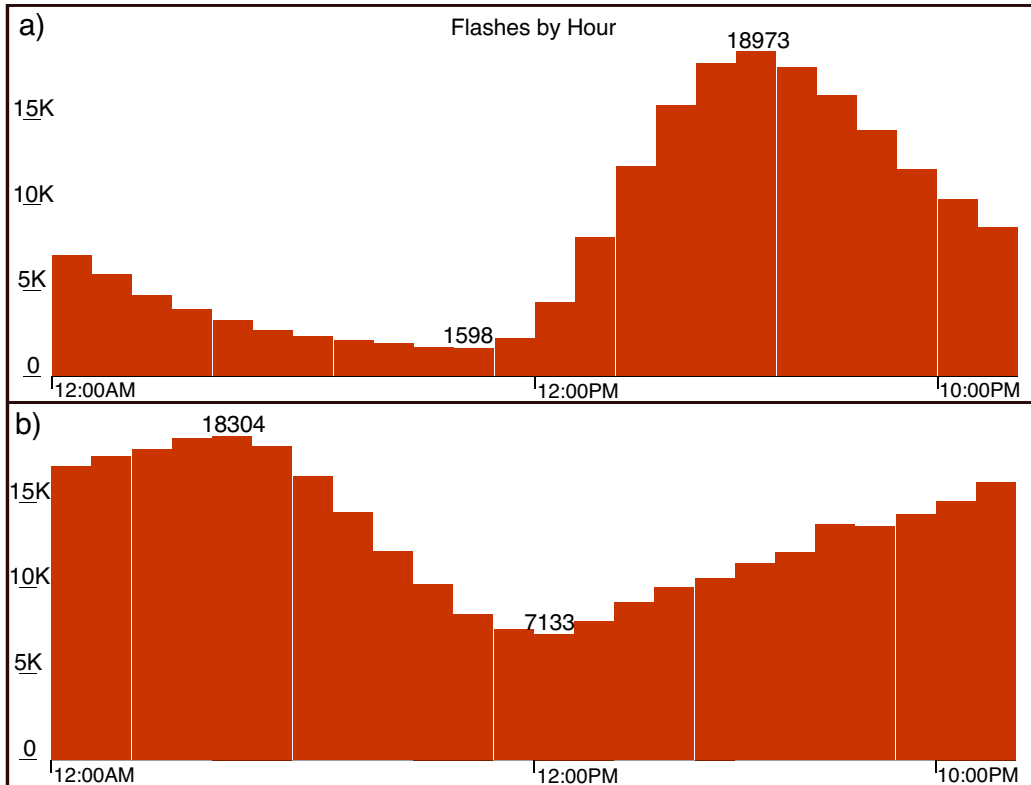


Fig. 3. a) Hourly distribution of flashes from 196,836 thunderstorms for the Washington, DC region (EDT). b) Hourly distribution of flashes from 310,209 thunderstorms for the Kansas City region (CDT).

aerosol type and loads, or more likely a combination of factors including aerosols and convective instability (Bell et al., 2009; Stallins et al., 2013; Yair et al., 2022).

3.3. Meteorological and aerosol environments

Numerous investigations have found positive relationships between CAPE, lightning, and thunderstorm activity (Williams et al., 2002; Pawar et al., 2012; Murugavel et al., 2014; Dewan et al., 2018; Sun et al., 2023; Wang et al., 2023a, 2023b). When examining the initiation environments of the thunderstorms identified, there exist statistically significant, positive relationships between CAPE and the flash counts of these thunderstorm events for both regions (Fig. 4a and b). The initiation environment for Washington, DC thunderstorms consists of lower CAPE than Kansas City for all flash categories. The Kansas City region also has 37% more thunderstorms than Washington, DC, likely due to the greater convective instability present in their initiation environments (Fig. 4). When examining the same afternoon period (12:00–8 pm) for both regions, the Kansas City region still has more thunderstorm occurrences – 29% more than Washington, DC. Given the statistically significant positive correlation between convective instability and thunderstorm flash counts, the potential of aerosols to influence the thunderstorm environments of both regions will need to simultaneously control for CAPE (Fan et al., 2007; Storer et al., 2010).

When examining the distribution of CAPE by PM2.5 concentration within the thunderstorm initiation environment, the Washington, DC

and Kansas City regions exhibit similar distributions (Fig. 5). Even though Washington, DC environments contain lower overall CAPE, the CAPE decreases at the highest category of PM2.5 similar to Kansas City (Fig. 5). Washington, DC has much higher concentrations of PM2.5 than Kansas City and a significant decrease in CAPE when PM2.5 concentrations are above $40 \mu \text{m}^{-3}$ as seen in the thunderstorm initiation environments (Fig. 5a). When PM2.5 concentrations are below $30 \mu \text{m}^{-3}$, the CAPE present in thunderstorm initiation environments is nearly uniform (Fig. 5a). Kansas City initiation environments illustrate a gradual increase in CAPE until PM2.5 concentrations reach over $30 \mu \text{m}^{-3}$, then evidence suggests convective instability begins to decrease possibly due to the partitioning of sunlight (Fig. 5b). There were no identified thunderstorm initiation environments with PM2.5 concentrations above $40 \mu \text{m}^{-3}$ in Kansas City. Both regions exhibit similar PM2.5 concentrations across thunderstorm flash counts (Fig. 6). For thunderstorms producing >1000 flashes, PM2.5 concentrations ranged from 0 to $36 \mu \text{m}^{-3}$ (7.2 and 9.1 medians, respectively, with narrow, right-skewed, interquartile ranges, $<12 \mu \text{m}^{-3}$) across both geographic regions (Fig. 6a and b). Greater overall variance in PM2.5 concentrations occurs across thunderstorms with lower flash counts. A Kruskal-Wallis test concluded that the differences in means of PM2.5 concentrations across flash categories were significant at a 95% confidence interval for both regions.

PM10 concentrations with respect to CAPE are reversed between the two regions when compared with PM2.5 (Fig. 7). The Kansas City, MO region has much higher PM10 amounts than Washington, DC with

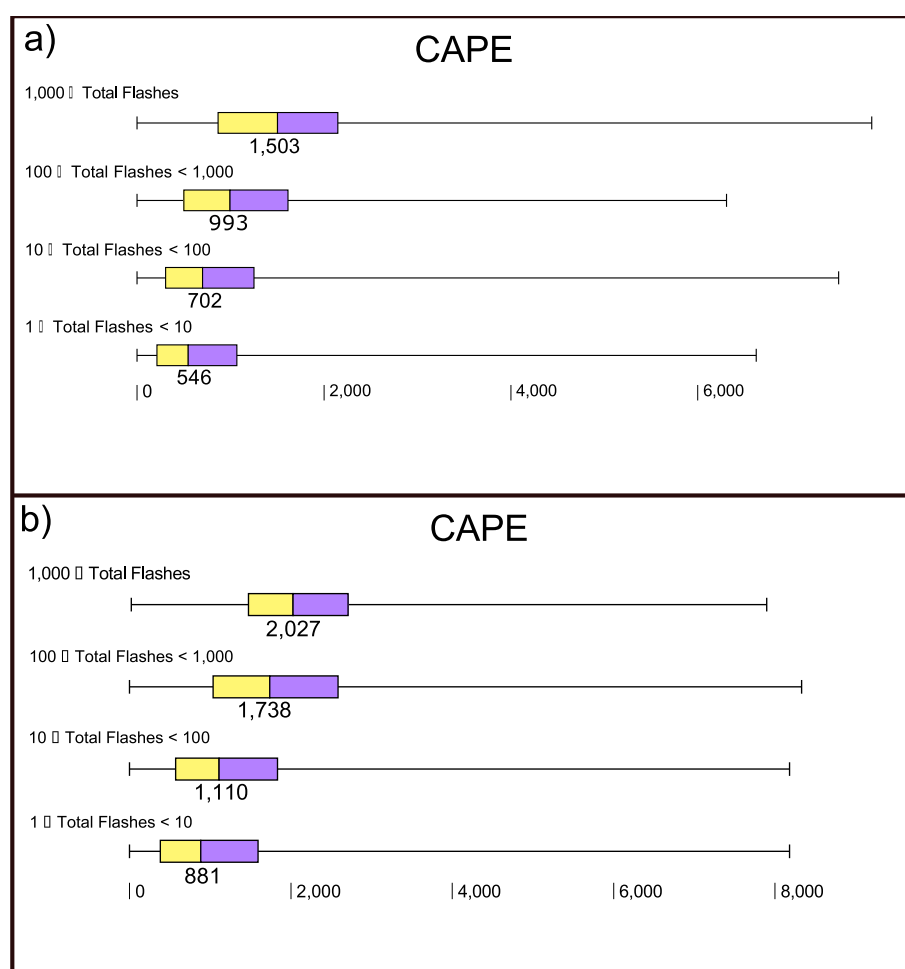


Fig. 4. a) Box plot with median values of CAPE (J kg^{-1}) by thunderstorm flashes for 194,186 thunderstorms in the Washington, DC region. b) Box plot with median values of CAPE (J kg^{-1}) by thunderstorm flashes for 105,714 thunderstorms occurring between noon and 8 pm in the Kansas City region. Both box plots exhibit statistically significant differences in medians between categories.

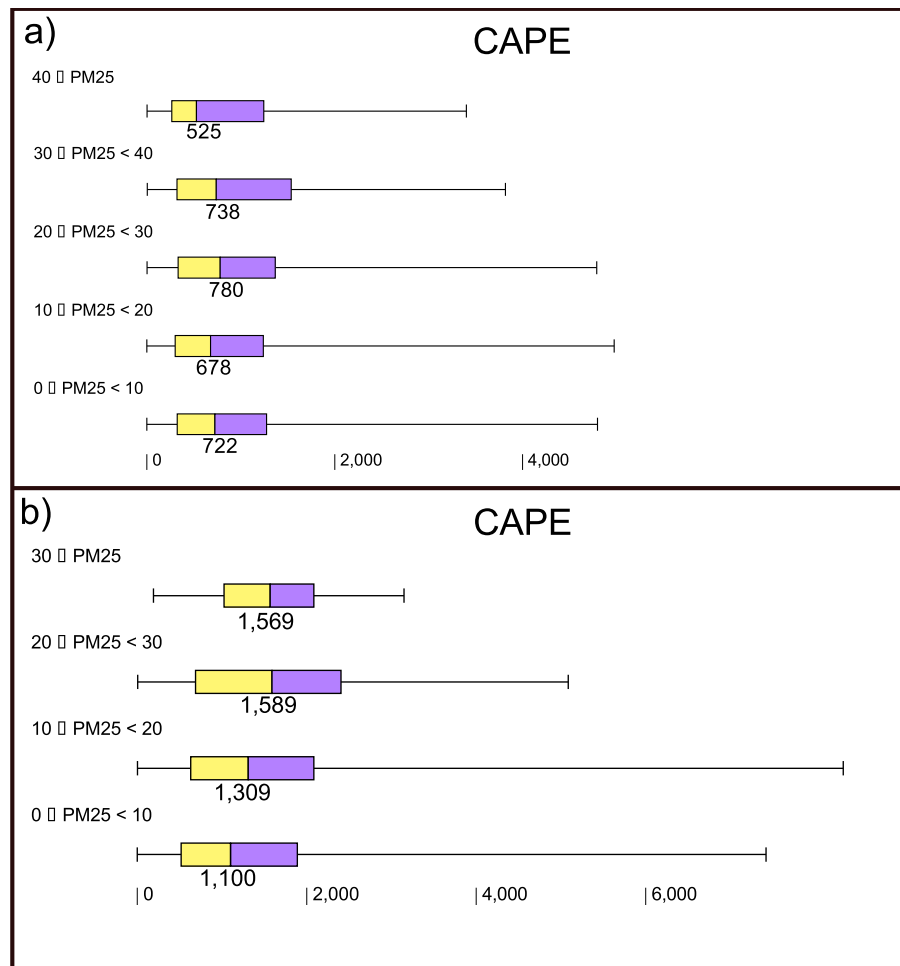


Fig. 5. a) Box plot with median values of CAPE (J kg^{-1}) by PM2.5 concentration for 18,393 thunderstorms in the Washington, DC region. b) Box plot with median values of CAPE (J kg^{-1}) by PM2.5 concentration for 3914 thunderstorms occurring between noon and 8 pm in the Kansas City region. Both box plots exhibit statistically significant differences in medians between categories.

concentrations surpassing $325 \mu \text{m}^{-3}$ (Fig. 7b). Washington, DC has lower PM10 concentrations than Kansas City and exhibits increasing CAPE throughout PM10 categories (Fig. 7a). Both regions exhibit restricted ranges in CAPE as PM10 concentrations increase (Fig. 7). Although CAPE increases through PM10 categories in the Washington, DC region, differences in CAPE are not statistically significant. Likewise, differences in CAPE across PM10 categories for Kansas City are also not statistically significant; however, it does appear instability is lower at PM10 concentrations above $200 \mu \text{m}^{-3}$ (Fig. 7b). When examining how thunderstorm flash counts vary across PM10 concentrations, similarities exist for thunderstorm events >1000 flashes for both regions (Fig. 8). They both have similar medians, narrow interquartile ranges (12 and $17 \mu \text{m}^{-3}$), and overall ranges (0 to $80 \mu \text{m}^{-3}$). For flash count categories below 1000, the regions have considerably more variance in PM10 concentrations, albeit similar medians (Fig. 8). For the Kansas City region, where PM10 concentrations are higher than Washington, DC, narrow, rightward skewing interquartile ranges are noted in all flash categories indicating the importance of relatively low PM10 concentrations in thunderstorm initiation environments across all categories (Fig. 8b). Statistically significant, unequal medians existed across both regions for all PM10 concentrations and event flash counts.

When comparing the overall aerosol/instability environment of thunderstorm initiation across both regions, Washington, DC has a much higher concentration of PM2.5 aerosols than Kansas City (Fig. 5). The PM2.5 concentration appears to reach a threshold high enough to negatively impact CAPE and suppress flash counts in thunderstorms

similar to previous findings of the influence of aerosol concentrations on lightning (Fig. 4a; Naccarato et al., 2003; Altaratz et al., 2010; Tan et al., 2016; Shi et al., 2020). For the Kansas City region, CAPE appears to be slightly suppressed, but still increases across PM2.5 concentration categories (Fig. 5b). The smaller range and lower medians of PM2.5 concentrations in high flash count thunderstorm events (> 1000 flashes) highlight the importance of aerosols in suppressing thunderstorm initiation and lightning production once a threshold amount is reached (Fig. 6). When examining PM10 concentrations, CAPE in the Washington, DC region does not appear suppressed given the lower amounts, especially when compared to the Kansas City region (Fig. 7). The CAPE distribution across the Kansas City region does appear to be limited by the much higher PM10 concentrations (Fig. 7b). Similar to PM2.5 aerosol concentrations, PM10 aerosols occur in a somewhat restricted range and low median during the initiation of large flash count events (> 1000 flashes; Fig. 8). Although median concentrations of PM10 aerosols are between 12 and $17 \mu \text{m}^{-3}$, a much wider range occurs across both regions in lower flash count categories, varying from 0 to nearly $600 \mu \text{m}^{-3}$ (Fig. 8). The lower concentrations and constricted ranges of PM2.5 and PM10 across both regions during initiation of high flash count thunderstorms (> 1000 flashes) highlight the importance of optimum aerosol quantities acting to promote convective instability and generate lightning.

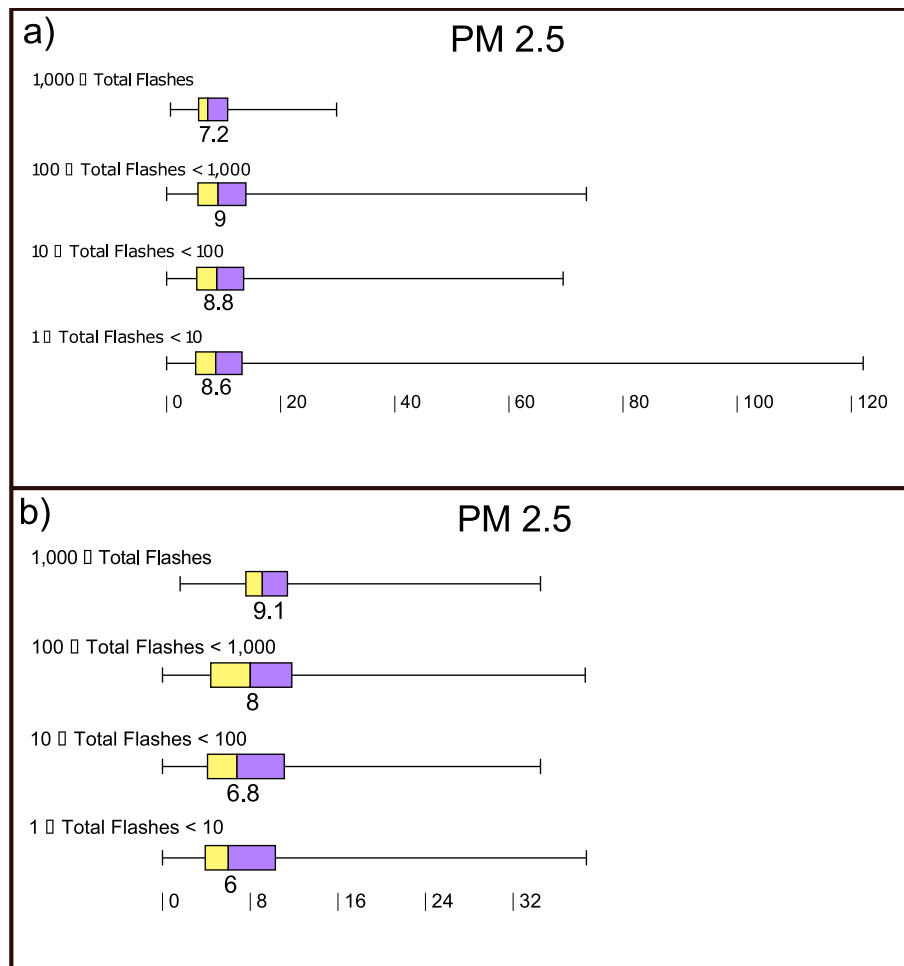


Fig. 6. a) Box plot with median values of PM2.5 concentration by total thunderstorm flashes for 18,393 thunderstorms in the Washington, DC region. b) Box plot with median values of PM2.5 concentration by total thunderstorm flashes for 3914 thunderstorms occurring between noon and 8 pm in the Kansas City region. Both box plots exhibit statistically significant differences in medians between categories.

3.4. Covariation of CAPE and aerosol environments

To further examine the relationships between particulate matter, CAPE, and flash counts, initiation regions were stratified by particulate matter concentration and then into four CAPE categories. Covariation between CAPE and aerosol quantities (AOD, PM10, and PM2.5) were analyzed by assigning data to four percentile-based bins using 50th, 75th and 90th percentiles as bin edges (Table 2).

For Washington, DC, in lower PM2.5 environments of <75% ($13.4 \mu\text{g m}^{-3}$), flash counts are maximized in thunderstorms initiating in CAPE environments >90% (Fig. 9a and b). In environments with PM2.5 concentrations >75%, CAPE amounts >90% (2206 J kg^{-1}) are required to produce higher flash count thunderstorms (Fig. 9c and d). The intermediate PM2.5 concentrations between 50 and 75% (8.7 and $13.4 \mu\text{g m}^{-3}$) produce thunderstorms with the highest flash counts across CAPE amounts >2206 J kg^{-1} (Fig. 9b; Pérez-Invernón et al., 2021). A similar distribution is noted for the Kansas City region (Fig. 10). For initiation environments with PM2.5 concentrations of between 50 and 75% (6.2 and $10 \mu\text{g m}^{-3}$) and CAPE amounts >90% (2533 J kg^{-1}), flash counts in thunderstorm events are maximized (Fig. 10b). In environments exhibiting PM2.5 concentrations of >90% ($19.3 \mu\text{g m}^{-3}$), flash counts in thunderstorms appear to be somewhat suppressed except in the highest CAPE percentile (Fig. 10d). Evidence suggests that high CAPE environments reinforce non-inductive charging which produces higher lightning flash rates, although results indicate moderate amounts of pollution act in concert with CAPE to maximize flash counts (Sun et al., 2023).

Stratifying by PM10, Washington, DC thunderstorms initiating in environments characterized by CAPE amounts >75% (1169 J kg^{-1}) exhibit the highest flash counts across all PM10 percentiles (Fig. 11). Thunderstorms initiating in CAPE >75% and PM10 environments >90% produce the highest flash counts, although a large range in flash counts exists within the >90% CAPE environments (Fig. 11d). For Kansas City thunderstorms, there is an increase in flash counts for thunderstorms initiating in CAPE environments >75% (1688 J kg^{-1}) across PM10 concentrations <90% ($31 \mu\text{g m}^{-3}$; Fig. 12). In fact, higher PM10 concentrations yield higher flash count thunderstorms across these categories (Fig. 12). For Kansas City, thunderstorms initiating in CAPE environments of >75% (1688 J kg^{-1}) appear most sensitive to PM10 concentrations with increasing amounts generating thunderstorms with more flashes until PM10 percentiles reach 90% ($31 \mu\text{g m}^{-3}$). Given that thunderstorms in the Kansas City region initiate in higher CAPE and lower PM10 environments than Washington, DC, it appears that flash rates in these thunderstorms are modulated by PM10 concentrations in higher CAPE environments (> 1688 J kg^{-1} ; Fig. 12).

The differences in thunderstorm flash counts in both regions appear to be correlated with the concentration of PM2.5 and PM10 found in the initiation regions of thunderstorms. Washington, DC environments contain higher amounts of PM2.5 than Kansas City. The Kansas City region initiation environments contain higher overall PM10 concentrations (Fig. 12). Evidence suggests that higher aerosol concentration does little to impact thunderstorm flash counts in environments with CAPE amounts of <75% (Figs. 9 and 12). Similar to prior research examining

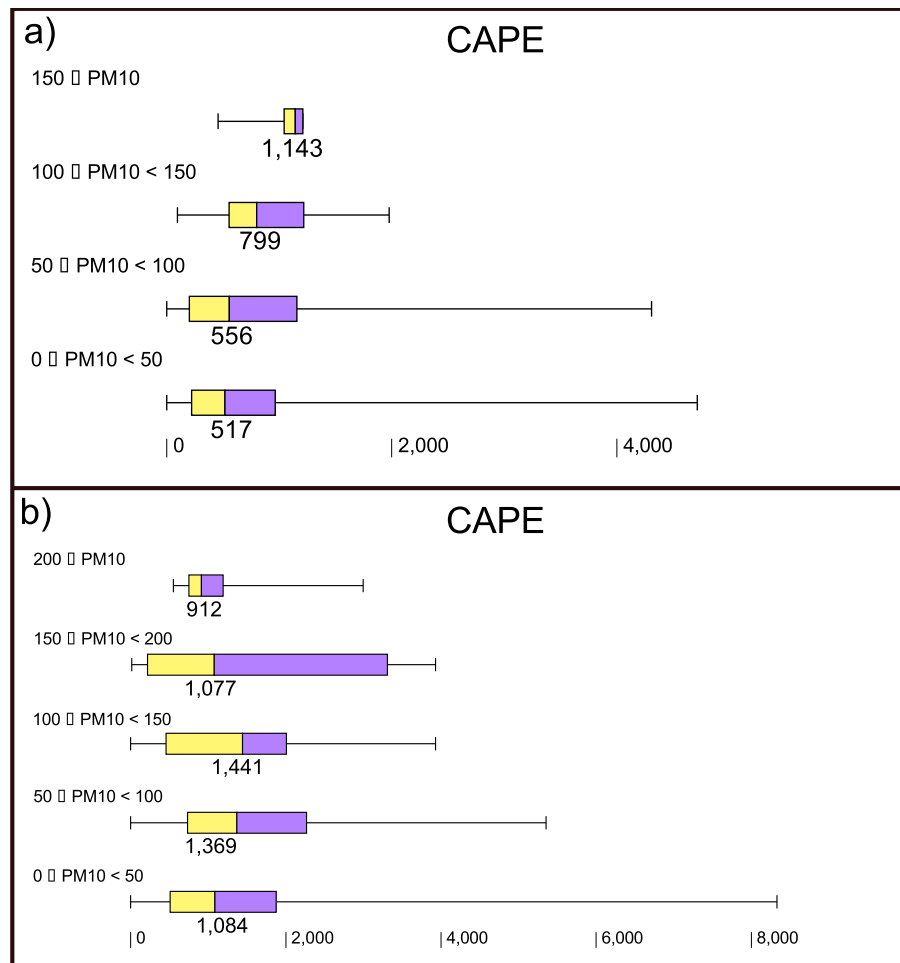


Fig. 7. a) Box plot with median values of CAPE (J kg^{-1}) by PM10 concentration for 10,446 thunderstorms in the Washington, DC region. b) Box plot with median values of CAPE by PM10 concentration for 14,943 thunderstorms occurring between noon and 8 pm in the Kansas City region. Both box plots exhibit statistically significant differences in medians between categories.

the relationship between CAPE and CCN, in CAPE environments $>75\%$, results suggest higher aerosol concentrations can enhance thunderstorm flash counts (Sun et al., 2023). For Washington, DC, PM2.5 concentrations up to 75% yield enhanced flash counts in thunderstorms initiating with CAPE amounts $>75\%$ and appear to suppress flash counts in thunderstorms initiating with lower CAPE amounts (Fig. 9). In the Kansas City region, PM10 concentrations up to 90% yield considerably higher flash counts in thunderstorms initiating in CAPE environments higher than 75% (Fig. 12). Evidence suggests that thunderstorms initiating in environments with CAPE amounts of at least 75% are the most sensitive to changes in aerosols regardless of size (Figs. 9 and 12; Sun et al., 2023). These results deviate from prior research that found additional CAPE did not enhance lightning activity in a moderate- to high-CCN environment (Hu et al., 2019). Our findings exemplify the importance of untangling the constructive and destructive interactions that occur between thermodynamics and aerosols in the initiation region of thunderstorms across both regions.

To further refine the examination of aerosol concentration and particle size, AOD and AE were analyzed with respect to CAPE and thunderstorm flash counts. Evidence of the “boomerang shape” in lightning production under different AODs exists (Wang et al., 2018). When stratifying the dataset by 500 nm AOD, it appears that the optical depth modulates flash counts the greatest within thunderstorms initiating in CAPE environments $>75\%$ (1169 J kg^{-1}) in Washington, DC (Fig. 13). Flash counts of thunderstorms gradually decrease as AOD percentiles increase (Fig. 13). Kansas City region thunderstorms are characterized

by lower AODs than Washington, DC (Table 2). However, flash counts in thunderstorms also appear to be sensitive to the AOD with flashes in thunderstorms maximized across all CAPE categories in AOD percentiles of 75 to 90% (Fig. 14). For AODs $>90\%$ (0.30), flash counts decrease in all CAPE categories (Fig. 14d).

For the Washington, DC region, thunderstorm initiation environments are characterized by AE decreasing with respect to increasing AOD (Fig. 15a). Decreasing AE indicates particles becoming coarser as hazier conditions occur. Kansas City environments are notably similar with AE decreasing as AOD increases, also indicating that hazier environments are characterized by larger particles (Fig. 15b). Their scatterplots are also similar in that many thunderstorm environments in both cities are clustered on the left-side of the scatterplot where AE values are <2 and AOD is <0.3 , indicating coarser particles and less hazy conditions (Fig. 15). When comparing thunderstorm initiation across AOD amounts, Washington, DC thunderstorms initiate in a wider range of conditions (Fig. 15). Kansas City thunderstorms initiate in AOD amounts primarily below 0.5 (Fig. 15b). The negative correlation between AE and AOD for both cities are statistically significant at the 0.05 alpha-level.

4. Conclusions

Evidence suggests that warm season thunderstorm environments in benign synoptic conditions are considerably different in thermodynamics, aerosol properties, and aerosol concentrations between the

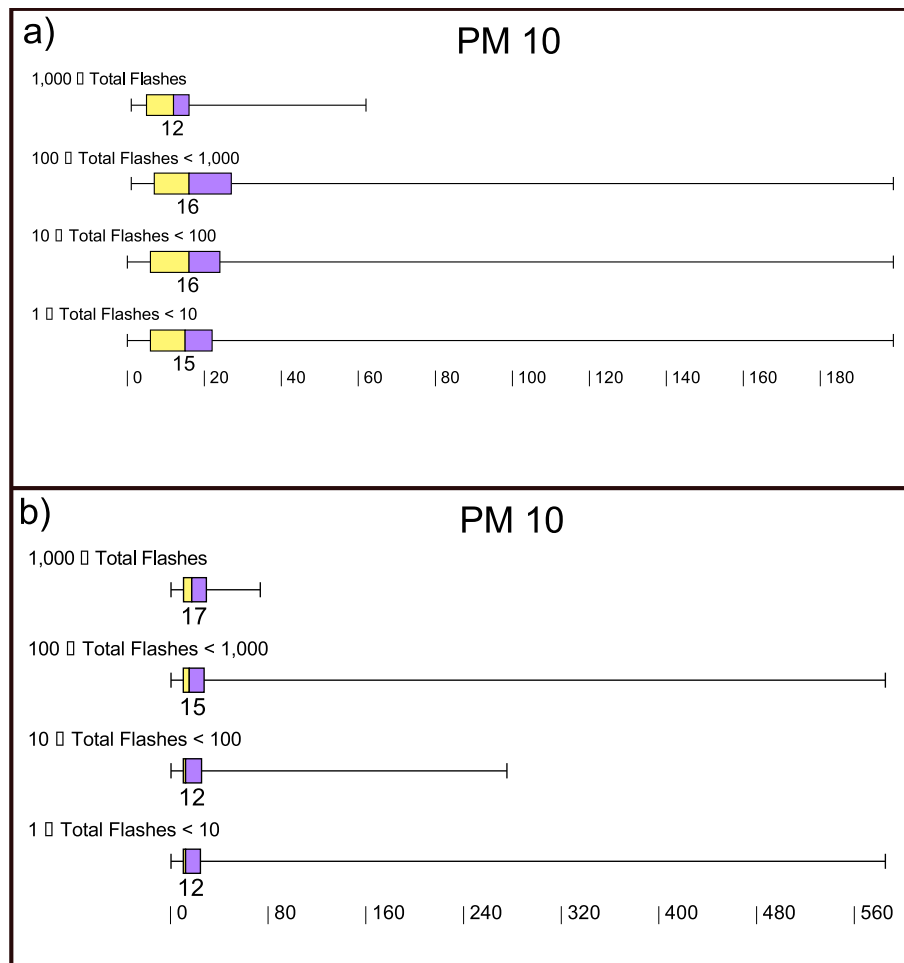


Fig. 8. a) Box plot with median values of PM10 concentration by total thunderstorm flashes for 10,446 thunderstorms in the Washington, DC region. b) Box plot with median values of PM10 concentration by total thunderstorm flashes for 14,943 thunderstorms occurring between noon and 8 pm in the Kansas City region. Both box plots exhibit statistically significant differences in medians between categories.

Table 2

Quantile statistics of PM2.5, PM10, AOD, CAPE, and events per flash for Washington, DC and Kansas City.

	City	0.25	0.5	0.75	0.9	0.95	1
CAPE (J kg^{-1})	DC	239	615	1169	1781	2206	7863
	KC	374	911	1688	2533	3071	9774
PM2.5 ($\mu\text{g m}^{-3}$)	DC	5.2	8.7	13.4	19.3	23.6	122.1
	KC	3.7	6.2	10	14.1	17.3	79
PM10 ($\mu\text{g m}^{-3}$)	DC	6	16	24	37	49	199
	KC	10	10.3	20	31	33	654
AOD 500 nm (-)	DC	0.19	0.28	0.42	0.61	0.82	1.60
	KC	0.12	0.16	0.23	0.30	0.32	0.99
Flashes per event	DC	2	5	21	87	174	7289
	KC	2	5	24	110	233	6169

Washington, DC and Kansas City regions. However, it appears that thunderstorm intensity, as measured by flash counts, is regulated by similar thermodynamic-aerosol relationships despite the differences in ambient environments. Specific findings from this investigation include:

- Washington, DC warm season thunderstorm occurrence follows a diurnal heating curve with the peak hour of thunderstorm initiation occurring at 4 pm. The Kansas City region exhibits an early evening peak in thunderstorm initiation, likely produced by diurnal heating; however, the early morning peak at 4 am is more persistent and lasts several hours from midnight onwards.

- Washington, DC exhibits the highest frequency of thunderstorm occurrence on Thursday. When removing the impact of nocturnal thunderstorms, Kansas City exhibits a similar day-of-the-week distribution. Thursday remains the peak day of thunderstorm occurrence, with secondary maxima occurring on Monday and Tuesday. This suggests that the variation in day-of-the-week thunderstorm occurrence in Washington, DC and during the afternoon in the Kansas City region are possibly tied to variability in aerosol loads.
- When examining the initiation environments of the thunderstorms identified, there exist statistically significant, positive relationships between CAPE and the flash counts of these events for both regions. The Kansas City region also contains 37% more thunderstorms than Washington, DC, likely due to the greater convective instability present in their initiation environments.
- Both regions exhibit similar PM2.5 concentrations across thunderstorm flash counts. For thunderstorms producing >1000 flashes, PM2.5 concentrations ranged from 0 to $36 \mu\text{g m}^{-3}$ (medians of 7.2 and 9.1 for the Washington, DC and Kansas City regions respectively), with narrow, right-skewed, interquartile ranges of $<12 \mu\text{g m}^{-3}$.
- For the Kansas City region, where PM10 concentrations are higher than Washington, DC, narrow, rightward-skewing interquartile ranges are noted in all flash categories, indicating the importance of relatively low PM10 concentrations in thunderstorm initiation environments. When comparing the overall aerosol/instability environments of thunderstorm initiation across both regions, Washington, DC has a much higher concentration of PM2.5 aerosols

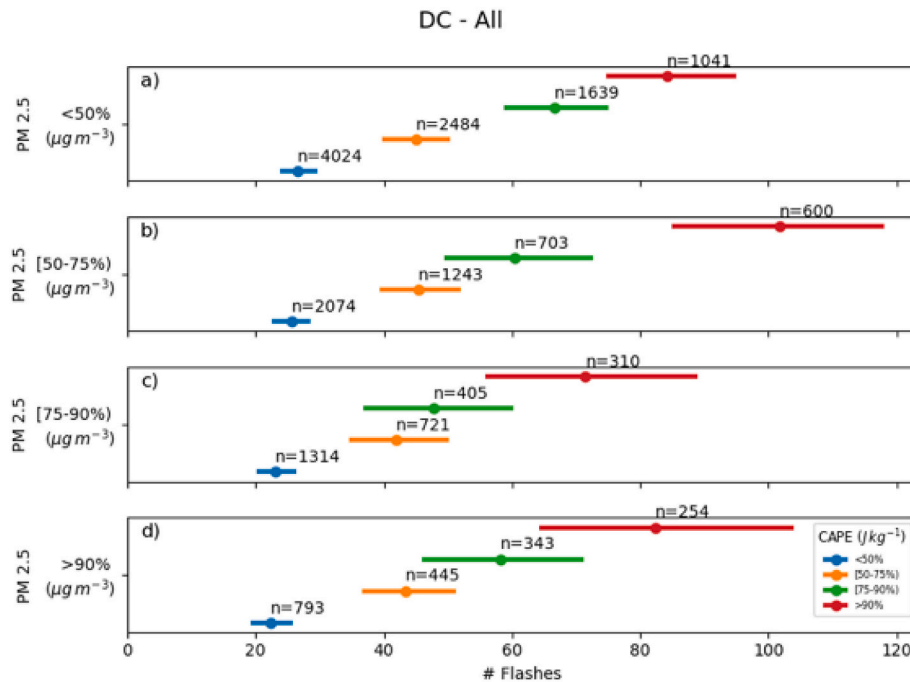


Fig. 9. Mean, sample size (n), and 95% confidence intervals for each PM2.5 quantile. a) Total thunderstorm flashes by CAPE ($J kg^{-1}$) quantiles for thunderstorms in the Washington, DC region stratified by PM2.5 concentrations of the <50% quantile. b) same as a), except for PM2.5 concentrations of between 50 and 75% quantiles. c) same as a), except for PM2.5 concentrations of between 75 and 90% quantiles. d) same as a), except for PM2.5 concentrations of the >90% quantile.

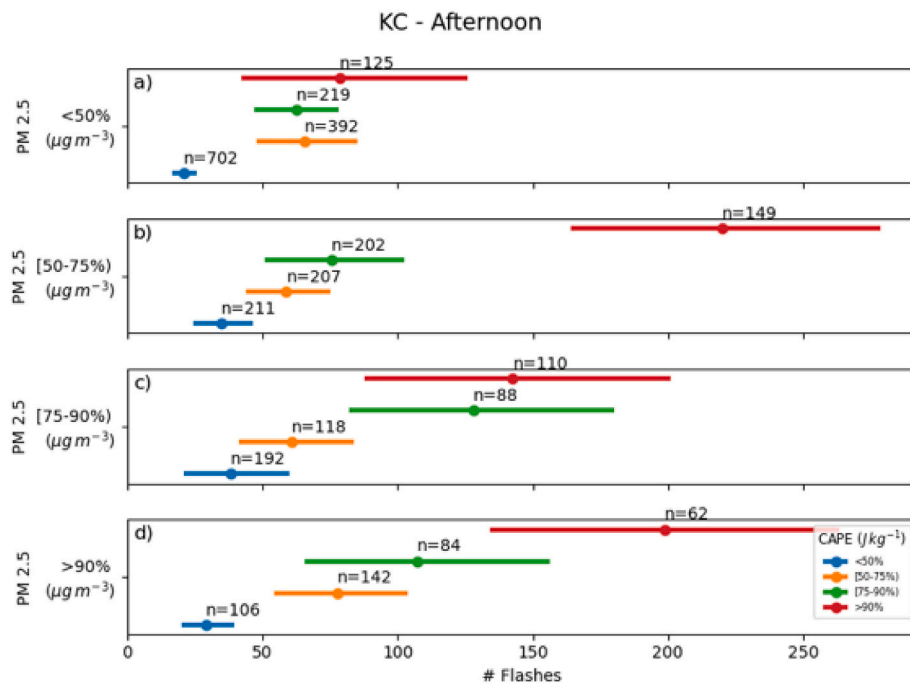


Fig. 10. Mean, sample size (n), and 95% confidence intervals for each PM2.5 quantile. a) Total thunderstorm flashes by CAPE ($J kg^{-1}$) quantiles for thunderstorms occurring between noon and 8 pm in the Kansas City region stratified by PM2.5 concentrations of the <50% quantile. b) same as a), except for PM2.5 concentrations of between 50 and 75% quantiles. c) same as a), except for PM2.5 concentrations of between 75 and 90% quantiles. d) same as a), except for PM2.5 concentrations of the >90% quantile.

and a much lower concentration of PM10 aerosols than Kansas City. The lower concentrations and constricted ranges of PM10 and PM2.5 across the Washington, DC and Kansas City regions, respectively, during initiation of high flash count events (> 1000 flashes) underlines the importance of optimum aerosol quantities acting in concert with CAPE to intensify thunderstorms and generate

lightning. Evidence suggests that aerosol concentration is a more important quantity than particle size for lightning augmentation.

- It appears that higher aerosol concentration (either PM2.5 or PM10) has minimal impacts on thunderstorm flash counts in environments with CAPE amounts less than the 75% quantile. However, thunderstorms initiating in environments with CAPE amounts greater than

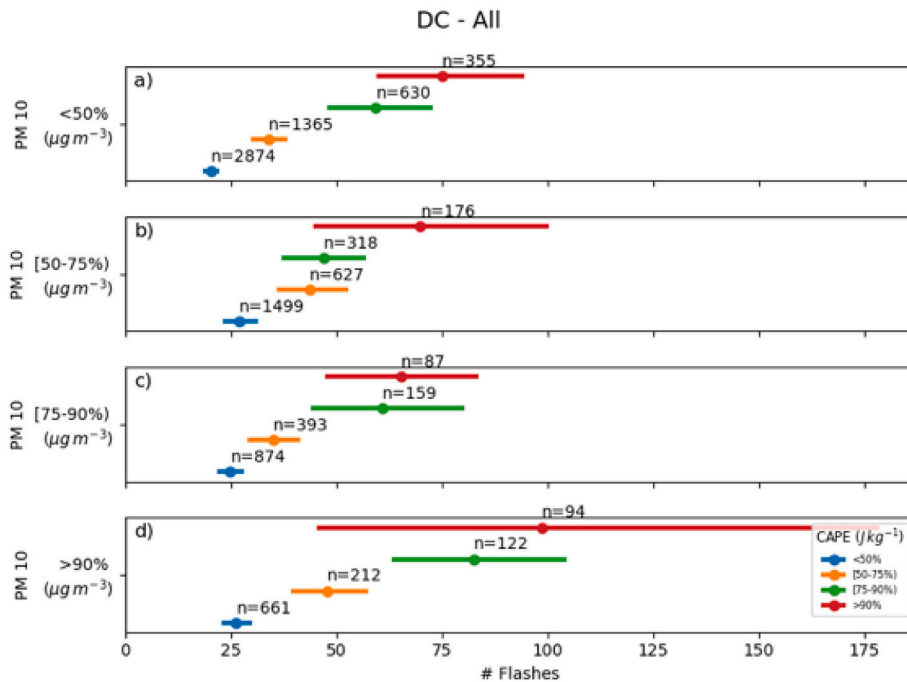


Fig. 11. Mean, sample size (n), and 95% confidence intervals for each PM10 quantile. a) Total thunderstorm flashes by CAPE (J kg^{-1}) quantiles for thunderstorms in the Washington, DC region stratified by PM10 concentrations of the <50% quantile. b) same as a), except for PM10 concentrations of between 50 and 75% quantiles. c) same as a), except for PM10 concentrations of between 75 and 90% quantiles. d) same as a), except for PM10 concentrations of the >90% quantile.

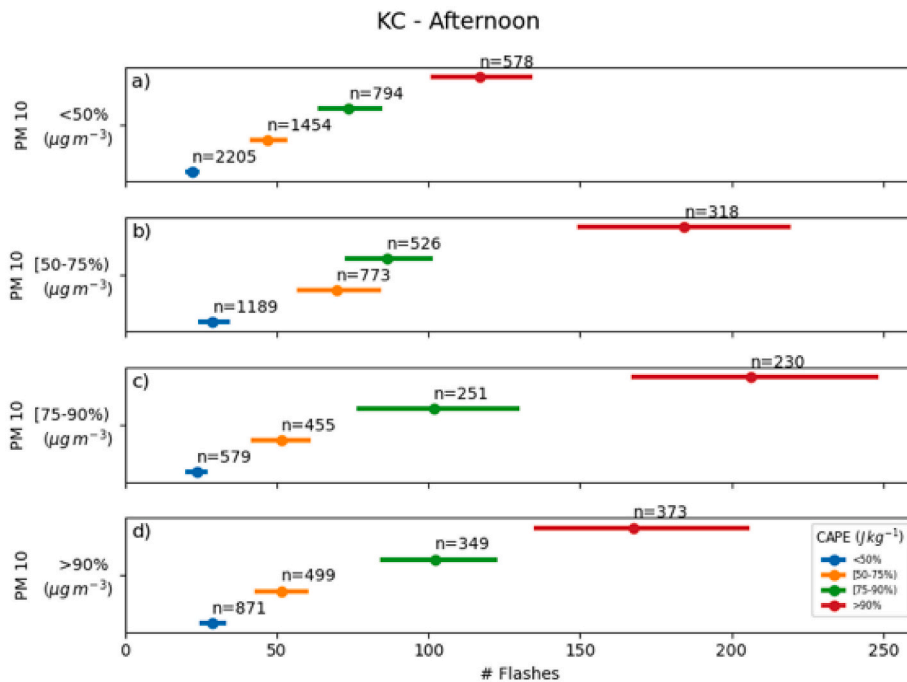


Fig. 12. Mean, sample size (n), and 95% confidence intervals for each PM10 quantile. a) Total thunderstorm flashes by CAPE (J kg^{-1}) quantiles for thunderstorms occurring between noon and 8 pm in the Kansas City region stratified by PM10 concentrations of the <50% quantile. b) same as a), except for PM10 concentrations of between 50 and 75% quantiles. c) same as a), except for PM10 concentrations of between 75 and 90% quantiles. d) same as a), except for PM10 concentrations of the >90% quantile.

the 75% quantile appear to be the most sensitive to changes in aerosols regardless of size, with increasing aerosol concentrations promoting higher flash counts until aerosol concentrations are greater than the 90% quantile.

- Flash counts in thunderstorms appear to be sensitive to the AOD, with flashes in thunderstorms increasing across all CAPE

environments as AOD increases up to the 90% quantile. For AODs greater than the 90% quantile, flash counts decrease in all CAPE categories, possibly due to the partitioning of sunlight.

Future research will entail a closer examination of thunderstorm initiation environments within the urban cores of Washington, DC and

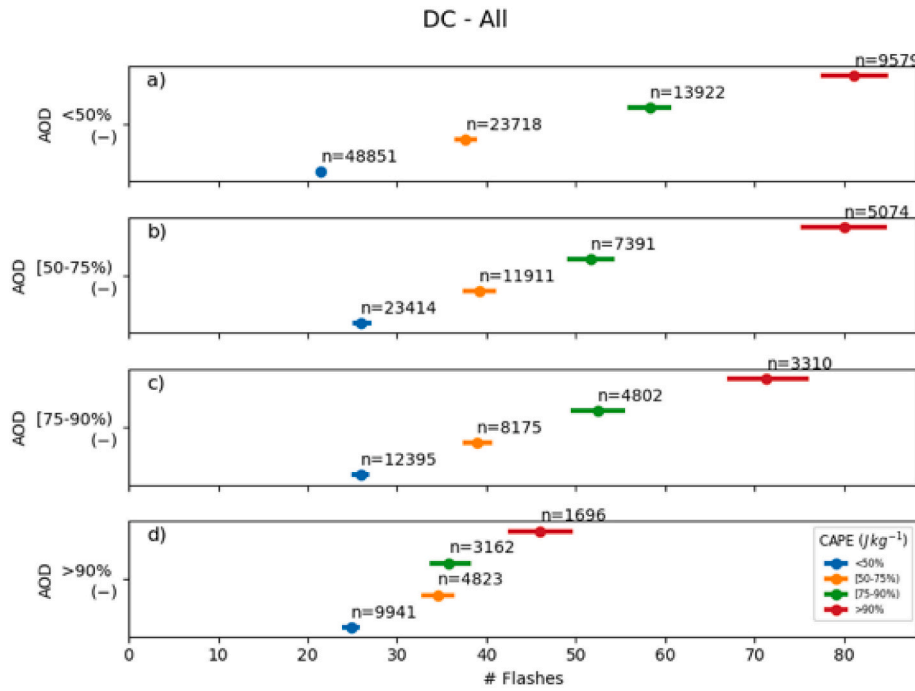


Fig. 13. Mean, sample size (n), and 95% confidence intervals for each 500 nm AOD quantile. a) Total thunderstorm flashes by CAPE ($J kg^{-1}$) quantiles for thunderstorms in the Washington, DC region stratified by 500 nm AOD of the <50% quantile. b) same as a), except for 500 nm AOD concentrations of between 50 and 75% quantiles. c) same as a), except for 500 nm AOD concentrations of between 75 and 90% quantiles. d) same as a), except for 500 nm AOD concentrations of the >90% quantile.

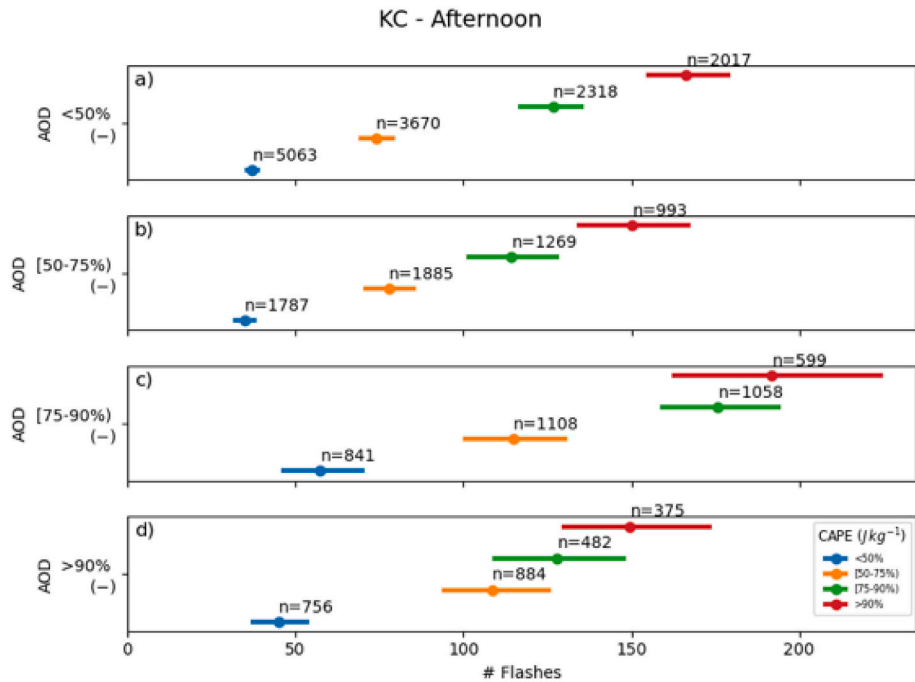


Fig. 14. Mean, sample size (n), and 95% confidence intervals for each 500 nm AOD quantile. a) Total thunderstorm flashes by CAPE ($J kg^{-1}$) quantiles for thunderstorms occurring between noon and 8 pm in the Kansas City region stratified by 500 nm AOD of the <50% quantile. b) same as a), except for 500 nm AOD concentrations of between 50 and 75% quantiles. c) same as a), except for 500 nm AOD concentrations of between 75 and 90% quantiles. d) same as a), except for 500 nm AOD concentrations of the >90% quantile.

Kansas City. The environments will be analyzed for differences between urban initiated thunderstorms versus those across the greater region to evaluate the impacts of pollution. Thunderstorm initiation locations will also be grouped by similar wind characteristics to identify differences in the upwind/downwind urban environments, thunderstorm

environments, and formation hotspots.

Funding

This work was supported by the National Science Foundation (Award

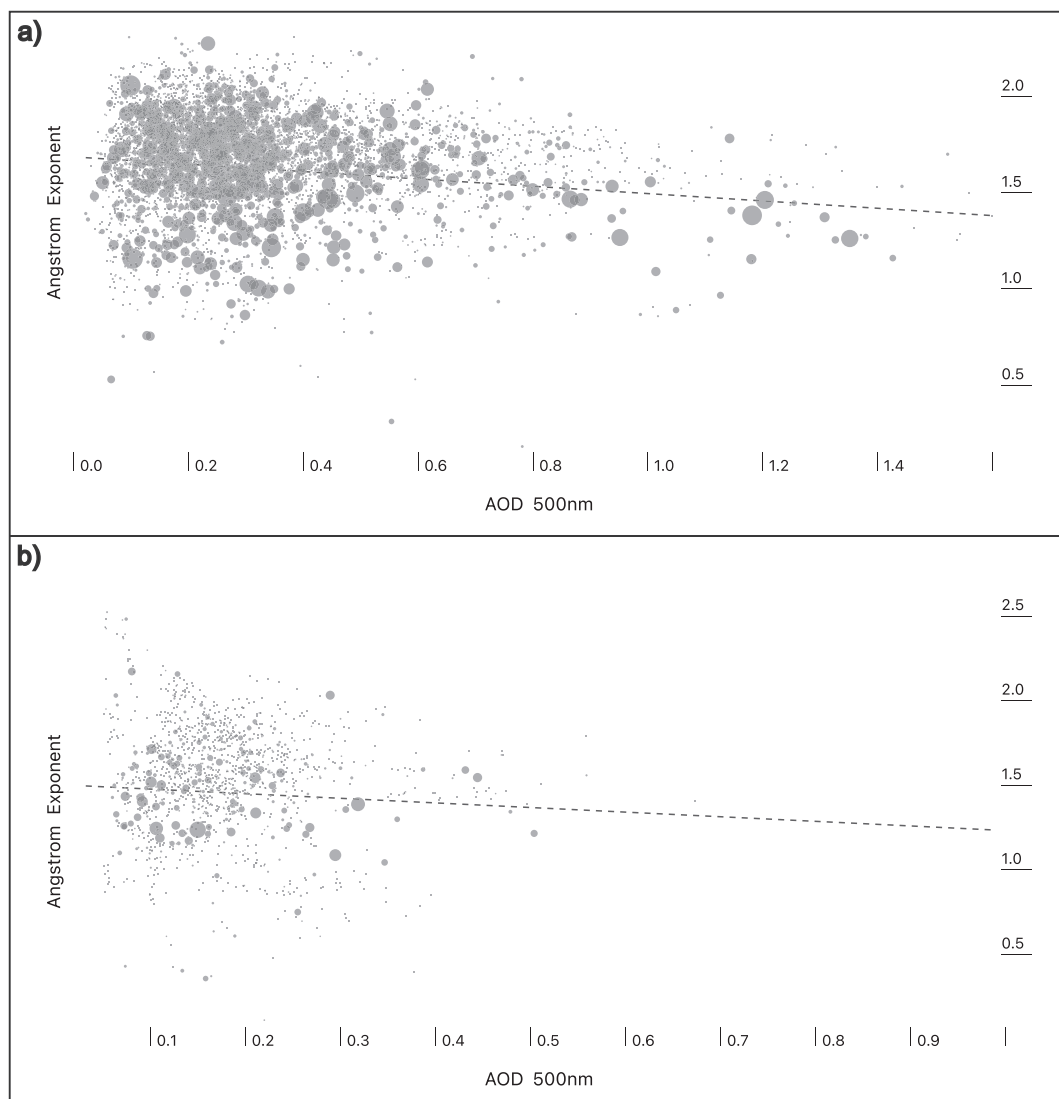


Fig. 15. a) Scatterplot with weighted markers of 440 - 675 nm Angstrom exponent by 500 nm AOD for 196,836 thunderstorms for the Washington, DC region. b) Scatterplot with weighted markers of 440 - 675 nm Angstrom exponent by 500 nm AOD for 25,100 thunderstorms occurring between noon and 8 pm for the Kansas City region. Both scatterplots have statistically significant correlations. Marker weights are based on frequency of occurrence for each value.

#2104299; 2021).

CRediT authorship contribution statement

Mace Bentley: Writing – review & editing, Writing – original draft, Visualization, Supervision, Project administration, Methodology, Investigation, Funding acquisition, Formal analysis, Conceptualization. **Tobias Gerken:** Visualization, Validation, Supervision, Software, Methodology, Investigation, Funding acquisition, Formal analysis, Data curation, Conceptualization, Writing – original draft, Writing – review & editing. **Zhuojun Duan:** Conceptualization, Data curation, Formal analysis, Funding acquisition, Investigation, Methodology, Project administration, Resources, Software, Supervision, Validation, Visualization. **Dudley Bonsal:** Data curation, Formal analysis, Funding acquisition, Investigation, Methodology, Project administration, Supervision, Visualization, Writing – original draft, Writing – review & editing. **Henry Way:** Writing – review & editing, Writing – original draft, Supervision, Resources, Project administration, Methodology, Investigation, Conceptualization, Funding acquisition. **Endre Szakal:** Visualization, Validation, Software, Resources, Data curation. **Mia Pham:** Validation, Software, Resources, Formal analysis, Data curation. **Hunter**

Donaldson: Visualization, Software, Formal analysis, Data curation. **Lucie Griffith:** Visualization, Software, Data curation.

Declaration of competing interest

The authors declare the following financial interests/personal relationships which may be considered as potential competing interests:

Mace Bentley reports financial support was provided by National Science Foundation.

Data availability statement

Due to NLDN's nature as a commercial dataset, we cannot share the underlying lightning data.

ERA5 data used in this research is available at: <https://cds.climate.copernicus.eu/cdsapp#!/dataset/reanalysis-era5-pressure-levels?tab=form>

AERONET data was downloaded from: <https://aeronet.gsfc.nasa.gov>
AQS data was downloaded from: https://aqs.epa.gov/aqsweb/airdata/download_files.html

Acknowledgements

The authors wish to thank the following students for assistance in the research that led to this manuscript: Hayden Abbott, Chelsea Lang, Allison Tucker, and Leah Wilczynski. The authors also wish to thank the four anonymous reviewers whose comments improved this manuscript.

References

Altaratz, O., Koren, I., Yair, Y., Price, C., 2010. Lightning response to smoke from Amazonian fires. *Geophys. Res. Lett.* 37 <https://doi.org/10.1029/2010GL042679>.

Altaratz, O., Koren, I., Remer, L.A., Hirsch, E., 2014. Review: Cloud invigoration by aerosols—coupling between microphysics and dynamics. *Atmos. Res.* 140–141, 38–60. <https://doi.org/10.1016/j.atmosres.2014.01.009>.

Anderson, T.L., Charlson, R.J., Winker, D.M., Ogren, J.A., Holmén, K., 2003. Mesoscale variations of tropospheric aerosols. *J. Atmos. Sci.* 60, 119–136. [https://doi.org/10.1175/1520-0469\(2003\)060<0119:MTOTA>2.0.CO;2](https://doi.org/10.1175/1520-0469(2003)060<0119:MTOTA>2.0.CO;2).

Andreae, M.O., 2004. Smoking rain clouds over the Amazon. *Science* 303, 1337–1342. <https://doi.org/10.1126/science.1092779>.

Arritt, R.W., Rink, T.D., Segal, M., Todey, D.P., Clark, C.A., Mitchell, M.J., Labas, K.M., 1997. The great plains low-level jet during the warm season of 1993. *Mon. Weather Rev.* 125, 2176–2192. [https://doi.org/10.1175/1520-0493\(1997\)125<2176:TPGLLJ>2.0.CO;2](https://doi.org/10.1175/1520-0493(1997)125<2176:TPGLLJ>2.0.CO;2).

Ashley, W.S., Bentley, M.L., Stallins, J.A., 2012. Urban-induced thunderstorm modification in the Southeast United States. *Clim. Chang.* 113, 481–498. <https://doi.org/10.1007/s10584-011-0324-1>.

Augustine, J.A., Caracena, F., 1994. Lower-Tropospheric Precursors to Nocturnal MCS Development over the Central United States. *Wea. Forecast.* 9, 116–135. [https://doi.org/10.1175/1520-0434\(1994\)009<0116:LTPTNM>2.0.CO;2](https://doi.org/10.1175/1520-0434(1994)009<0116:LTPTNM>2.0.CO;2).

Bang, S.D., Zipser, E.J., 2016. Seeking reasons for the differences in size spectra of electrified storms over land and ocean: seeking reasons for differences in size spectra. *J. Geophys. Res. Atmos.* 121, 9048–9068. <https://doi.org/10.1002/2016JD025150>.

Banta, R.M., Newsom, R.K., Lundquist, J.K., Pichugina, Y.L., Coulter, R.L., Mahrt, L., 2002. Nocturnal low-level jet characteristics over Kansas during Cases-99. *Bound.-Layer Meteorol.* 105, 221–252. <https://doi.org/10.1023/A:1019992330866>.

Bell, T.L., Rosenfeld, D., Kim, K.-M., 2009. Weekly cycle of lightning: evidence of storm invigoration by pollution. *Geophys. Res. Lett.* 36, L23805. <https://doi.org/10.1029/2009GL040915>.

Bentley, M.L., Ashley, W.S., Stallins, J.A., 2010. Climatological radar delineation of urban convection for Atlanta, Georgia. *Int. J. Climatol.* 30, 1589–1594. <https://doi.org/10.1002/joc.2020>.

Blanchard, D.O., 1998. Assessing the vertical distribution of convective available potential energy. *Wea. Forecast.* 13, 870–877. [https://doi.org/10.1175/1520-0434\(1998\)013<0870:ATVDOC>2.0.CO;2](https://doi.org/10.1175/1520-0434(1998)013<0870:ATVDOC>2.0.CO;2).

Carrión, G.G., Cotton, W.R., 2011. Urban growth and aerosol effects on convection over Houston. Part II: dependence of aerosol effects on instability. *Atmos. Res.* 102, 167–174. <https://doi.org/10.1016/j.atmosres.2011.06.022>.

Carrión, G.G., Cotton, W.R., Cheng, W.Y.Y., 2010. Urban growth and aerosol effects on convection over Houston. *Atmos. Res.* 96, 560–574. <https://doi.org/10.1016/j.atmosres.2010.01.005>.

Christian, H.J., 2003. Global frequency and distribution of lightning as observed from space by the Optical Transient Detector. *J. Geophys. Res.* 108, 4005. <https://doi.org/10.1029/2002JD002347>.

Coquillat, S., Bousseton, M.-P., Buguet, M., Lambert, D., Ribaud, J.-F., Berthelot, A., 2013. Lightning ground flash patterns over Paris area between 1992 and 2003: Influence of pollution? *Atmos. Res.* 122, 77–92. <https://doi.org/10.1016/j.atmosres.2012.10.032>.

Cotton, W.R., Anthes, R.A., 1989. *Storm and Cloud Dynamics, International Geophysics Series*. Academic press, San Diego New York Boston [etc.].

Craven, J.P., Brooks, H.E., 2004. Baseline climatology of sounding derived parameters associated with deep moist convection. *Natl. Wea. Dig.* 28, 13–24.

Cummins, K.L., Murphy, M.J., Bardo, E.A., Hiscox, W.L., Pyle, R.B., Pifer, A.E., 1998. A combined TOA/MDF technology upgrade of the U.S. National Lightning Detection Network. *J. Geophys. Res.* 103, 9035–9044. <https://doi.org/10.1029/98JD00153>.

Dewan, A., Onge, E.T., Rafiuddin, M., Rahman, Md.M., Mahmood, R., 2018. Lightning activity associated with precipitation and CAPE over Bangladesh: lightning in bangladesh. *Int. J. Climatol.* 38, 1649–1660. <https://doi.org/10.1002/joc.5286>.

Diem, J.E., Hursey, M.A., Morris, I.R., Murray, A.C., Rodriguez, R.A., 2010. Upper-level atmospheric circulation patterns and ground-level ozone in the Atlanta Metropolitan Area. *J. Appl. Meteorol. Climatol.* 49, 2185–2196. <https://doi.org/10.1175/2010JAMC2454.1>.

Dixon, P.G., Mote, T.L., 2003. Patterns and causes of Atlanta's urban heat island-initiated precipitation. *J. Appl. Meteorol.* 42, 1273–1284. [https://doi.org/10.1175/1520-0450\(2003\)042<1273:PACAO>2.0.CO;2](https://doi.org/10.1175/1520-0450(2003)042<1273:PACAO>2.0.CO;2).

Ekman, A.M.L., Engström, A., Söderberg, A., 2011. Impact of two-way aerosol–cloud interaction and changes in aerosol size distribution on simulated aerosol-induced deep convective cloud sensitivity. *J. Atmos. Sci.* 68, 685–698. <https://doi.org/10.1175/2010JAS3651.1>.

Emanuel, K.A., 1994. *Atmospheric Convection*. Oxford University Press, New York.

Fan, J., Zhang, R., Li, G., Tao, W.-K., 2007. Effects of aerosols and relative humidity on cumulus clouds. *J. Geophys. Res.* 112, D14204. <https://doi.org/10.1029/2006JD008136>.

Fan, J., Zhang, R., Tao, W.-K., Mohr, K.I., 2008. Effects of aerosol optical properties on deep convective clouds and radiative forcing. *J. Geophys. Res.* 113 (D8) <https://doi.org/10.1029/2007JD009257>.

Fan, F., Mann, M.E., Ammann, C.M., 2009. Understanding changes in the Asian summer monsoon over the past millennium: insights from a long-term coupled model simulation. *J. Clim.* 22, 1736–1748. <https://doi.org/10.1175/2008JCLI2336.1>.

Fan, J., Leung, L.R., Rosenfeld, D., Chen, Q., Li, Z., Zhang, J., Yan, H., 2013. Microphysical effects determine macrophysical response for aerosol impacts on deep convective clouds. *Proc. Natl. Acad. Sci.* 110, E4581–E4590. <https://doi.org/10.1073/pnas.1316830110>.

Fuchs, B.R., Rutledge, S.A., Bruning, E.C., Pierce, J.R., Kodros, J.K., Lang, T.J., MacGorman, D.R., Krehbiel, P.R., Rison, W., 2015. Environmental controls on storm intensity and charge structure in multiple regions of the continental United States: storm environmental controls. *J. Geophys. Res. Atmos.* 120, 6575–6596. <https://doi.org/10.1002/2015JD023271>.

Green, M., Kondragunta, S., Ciren, P., Xu, C., 2009. Comparison of GOES and MODIS Aerosol Optical Depth (AOD) to Aerosol Robotic Network (AERONET) AOD and IMPROVE PM 2.5 Mass at Bondville, Illinois. *J. Air Waste Manage. Assoc.* 59, 1082–1091. <https://doi.org/10.3155/1047-3289.59.9.1082>.

Guo, J., Liu, H., Li, Z., Rosenfeld, D., Jiang, M., Xu, W., et al., 2018. Aerosol-induced changes in the vertical structure of precipitation: a perspective of TRMM precipitation radar. *Atmos. Chem. Phys.* 18 (18), 13329–13343. <https://doi.org/10.5194/acp-18-13329-2018>.

Hersbach, H., Bell, B., Berrisford, P., Hirahara, S., Horányi, A., Muñoz-Sabater, J., Nicolas, J., Peubey, C., Radu, R., Schepers, D., Simmons, A., Soci, C., Abdalla, S., Abellán, X., Balsamo, G., Bechtold, P., Biavati, G., Bidlot, J., Bonavita, M., Chiara, G., Dahlgren, P., Dee, D., Diamantakis, M., Dragani, R., Flemming, J., Forbes, R., Fuente, M., Geer, A., Haimberger, L., Healy, S., Hogan, R.J., Hölm, E., Janisková, M., Keeley, S., Laloyaux, P., Lopez, P., Lupu, C., Radnoti, G., Rosnay, P., Rozum, I., Vamborg, F., Villaume, S., Thépaut, J., 2020. The ERA5 global reanalysis. *Q.J.R. Meteorol. Soc.* 146, 1999–2049. <https://doi.org/10.1002/qj.3803>.

Higgins, R.W., Yao, Y., Wang, X.L., 1997. Influence of the North American monsoon system on the U.S. Summer precipitation regime. *J. Clim.* 10, 2600–2622. [https://doi.org/10.1175/1520-0442\(1997\)010<2600:ITNAM>2.0.CO;2](https://doi.org/10.1175/1520-0442(1997)010<2600:ITNAM>2.0.CO;2).

Hu, J., Rosenfeld, D., Ryzhkov, A., Zrnic, D., Williams, E., Zhang, P., Snyder, J.C., Zhang, R., Weitz, R., 2019. Polarimetric radar convective cell tracking reveals large sensitivity of cloud precipitation and electrification properties to CCN. *JGR-Atmos.* 124, 12194–12205. <https://doi.org/10.1029/2019JD030857>.

Huang, T., Zhu, Y., Rosenfeld, D., Yang, Y., Lam, D.H.Y., Leung, W.H., et al., 2022. Regime-dependent impacts of aerosol particles and updrafts on the cloud condensation nuclei and the enhanced warm rain suppression: evidence from synergistic satellite and LiDAR observations. *Geophys. Res. Lett.* 49 <https://doi.org/10.1029/2021GL097315> e2021GL097315.

Igel, M.R., van den Heever, S.C., 2015. Tropical, oceanic, deep convective cloud morphology as observed by CloudSat (preprint). In: *Clouds and Precipitation/Remote Sensing/Troposphere/Physics (Physical Properties and Processes)*. <https://doi.org/10.5194/acpd-15-15977-2015>.

James, G., Witten, D., Hastie, T., Tibshirani, R., 2013. *An Introduction to Statistical Learning: With Applications in R*. Springer, New York.

Keim, B., Meeker, L., Slater, J., 2005. Manual synoptic climate classification for the east coast of New England (USA) with an application to PM2.5 concentration. *Clim. Res.* 28, 143–153. <https://doi.org/10.3354/cr028143>.

Khain, A., Rosenfeld, D., Pokrovsky, A., 2005. Aerosol impact on the dynamics and microphysics of deep convective clouds. *Q. J. R. Meteorol. Soc.* 131, 2639–2663. <https://doi.org/10.1256/qj.04.62>.

Khain, A.P., BenMoshe, N., Pokrovsky, A., 2008. Factors determining the impact of aerosols on surface precipitation from clouds: an attempt at classification. *J. Atmos. Sci.* 65, 1721–1748. <https://doi.org/10.1175/2007JAS2515.1>.

Kingfield, D.M., Calhoun, K.M., De Beurs, K.M., Henebry, G.M., 2018. Effects of city size on thunderstorm evolution revealed through a multiradar climatology of the central United States. *J. Appl. Meteorol. Climatol.* 57, 295–317. <https://doi.org/10.1175/JAMC-D-16-0341.1>.

Konwar, M., Mahes Kumar, R.S., Kulkarni, J.R., Freud, E., Goswami, B.N., Rosenfeld, D., 2012. Aerosol control on depth of warm rain in convective clouds. *J. Geophys. Res.* 117 (D13) <https://doi.org/10.1029/2012JD017585>.

Koren, I., Martins, J.V., Remer, L.A., Aafargan, H., 2008. Smoke invigoration versus inhibition of clouds over the Amazon. *Science* 321, 946–949. <https://doi.org/10.1126/science.1159185>.

Koren, I., Remer, L.A., Altaratz, O., Martins, J.V., Davidi, A., 2010. Aerosol-induced changes of convective cloud anvils produce strong climate warming. *Atmos. Chem. Phys.* 10, 5001–5010. <https://doi.org/10.5194/acp-10-5001-2010>.

Koren, I., Altaratz, O., Remer, L.A., Feingold, G., Martins, J.V., Heiblum, R.H., 2012. Aerosol-induced intensification of rain from the tropics to the mid-latitudes. *Nat. Geosci.* 5, 118–122. <https://doi.org/10.1038/ngeo1364>.

Li, B., Yuan, H., Feng, N., Tao, S., 2009. Comparing MODIS and AERONET aerosol optical depth over China. *Int. J. Remote Sens.* 30, 6519–6529. <https://doi.org/10.1080/0143160903111069>.

Li, Z., Rosenfeld, D., Fan, J., 2017. Aerosols and their impact on radiation, clouds, precipitation, and severe weather events. In: *Oxford Research Encyclopedia of Environmental Science*. Oxford University Press. <https://doi.org/10.1093/acrefore/9780199389414.013.126>.

Li, X., Pan, Y., Mo, Z., 2018. Joint effects of several factors on cloud-to-ground lightning and rainfall in Nanning (China). *Atmos. Res.* 212, 23–32. <https://doi.org/10.1016/j.atmosres.2018.05.002>.

Lopez, P., 2016. A lightning parameterization for the ECMWF integrated forecasting system. *Mon. Weather Rev.* 144, 3057–3075. <https://doi.org/10.1175/MWR-D-16-0026.1>.

Morales Rodriguez, C.A., da Rocha, R.P., Bombardi, R., 2010. On the development of summer thunderstorms in the city of São Paulo: mean meteorological characteristics and pollution effect. *Atmos. Res.* 96, 477–488. <https://doi.org/10.1016/j.atmosres.2010.02.007>.

Murugavel, P., Pawar, S.D., Gopalakrishnan, V., 2014. Climatology of lightning over Indian region and its relationship with convective available potential energy. *Int. J. Climatol.* 34, 3179–3187. <https://doi.org/10.1002/joc.3901>.

Naccarato, K.P., Pinto, O., Pinto, I.R.C.A., 2003. Evidence of thermal and aerosol effects on the cloud-to-ground lightning density and polarity over large urban areas of Southeastern Brazil: urban effects on CG lightning. *Geophys. Res. Lett.* 30 <https://doi.org/10.1029/2003GL017496>.

Orville, R.E., Huffines, G.R., 2001. Cloud-to-Ground Lightning in the United States: NLDN results in the first Decade, 1989–98. *Mon. Weather Rev.* 129, 1179–1193. [https://doi.org/10.1175/1520-0493\(2001\)129<1179:CTGLIT>2.0.CO;2](https://doi.org/10.1175/1520-0493(2001)129<1179:CTGLIT>2.0.CO;2).

Pawar, S.D., Lal, D.M., Murugavel, P., 2012. Lightning characteristics over Central India during Indian summer monsoon. *Atmos. Res.* 106, 44–49. <https://doi.org/10.1016/j.atmosres.2011.11.007>.

Pérez-Invernón, F.J., Huntrieser, H., Gordillo-Vázquez, F.J., Soler, S., 2021. Influence of the COVID-19 lockdown on lightning activity in the Po Valley. *Atmos. Res.* 263, 105808 <https://doi.org/10.1016/j.atmosres.2021.105808>.

Petersen, W.A., Rutledge, S.A., 2001. Regional variability in tropical convection: observations from TRMM. *J. Clim.* 14, 3566–3586. [https://doi.org/10.1175/1520-0442\(2001\)014<3566:RVITCO>2.0.CO;2](https://doi.org/10.1175/1520-0442(2001)014<3566:RVITCO>2.0.CO;2).

Power, H.C., 2003. The geography and climatology of aerosols. *Prog. Phys. Geogr. Earth Environ.* 27, 502–547. <https://doi.org/10.1191/030913303pp393ra>.

Power, H.C., Sheridan, S.C., Senkbeil, J.C., 2006. Synoptic climatological influences on the spatial and temporal variability of aerosols over North America. *Int. J. Climatol.* 26, 723–741. <https://doi.org/10.1002/joc.1277>.

Reynolds, S.E., Brook, M., Gourley, M.F., 1957. Thunderstorm charge separation. *J. Meteorol.* 14, 426–436. [https://doi.org/10.1175/1520-0469\(1957\)014<0426:TCS>2.0.CO;2](https://doi.org/10.1175/1520-0469(1957)014<0426:TCS>2.0.CO;2).

Rose, L.S., Stallins, J.A., Bentley, M.L., 2008. Concurrent cloud-to-ground lightning and precipitation enhancement in the Atlanta, Georgia (United States), urban region. *Earth Interact.* 12, 1–30. <https://doi.org/10.1175/2008EI265.1>.

Rosenfeld, D., Lensky, I.M., 1998. Satellite-based insights into precipitation formation processes in continental and maritime convective clouds. *Bull. Amer. Meteor. Soc.* 79, 2457–2476. [https://doi.org/10.1175/1520-0477\(1998\)079<2457:SBIIPF>2.0.CO;2](https://doi.org/10.1175/1520-0477(1998)079<2457:SBIIPF>2.0.CO;2).

Rosenfeld, D., Lahav, R., Khain, A., Pinsky, M., 2002. The role of sea spray in cleansing air pollution over ocean via cloud processes. *Science* 297, 1667–1670. <https://doi.org/10.1126/science.1073869>.

Rosenfeld, D., Lohmann, U., Raga, G.B., O'Dowd, C.D., Kulmala, M., Fuzzi, S., Reissell, A., Andreae, M.O., 2008. Flood or drought: how do aerosols affect precipitation? *Science* 321, 1309–1313. <https://doi.org/10.1126/science.1160606>.

Rosenfeld, D., Andreae, M.O., Asmi, A., Chin, M., de Leeuw, G., Donovan, D.P., Kahn, R., Kinne, S., Kivekäs, N., Kulmala, M., Lau, W., Schmidt, K.S., Suni, T., Wagner, T., Wild, M., Quaas, J., 2014. Global observations of aerosol-cloud-precipitation-climate interactions: aerosol-cloud-climate interactions. *Rev. Geophys.* 52, 750–808. <https://doi.org/10.1002/2013RG000441>.

Rosenfeld, D., Zheng, Y., Hashimshoni, E., Pöhler, M.L., Jefferson, A., Pöhler, C., et al., 2016. Satellite retrieval of cloud condensation nuclei concentrations by using clouds as CCN chambers. *Proc. Natl. Acad. Sci.* 113 (21), 5828–5834. <https://doi.org/10.1073/pnas.1514044113>.

Rosenfeld, D., Zhu, Y., Wang, M., Zheng, Y., Goren, T., Yu, S., 2019. Aerosol-driven droplet concentrations dominate coverage and water of oceanic low-level clouds. *Science* 363 (6427). <https://doi.org/10.1126/science.aav0566>.

Rudlosky, S.D., Fuelberg, H.E., 2010. Pre- and postupgrade distributions of NLDN reported cloud-to-ground lightning characteristics in the contiguous United States. *Mon. Weather Rev.* 138, 3623–3633. <https://doi.org/10.1175/2010MWR3283.1>.

Schmid, P.E., Niyogi, D., 2017. Modeling urban precipitation modification by spatially heterogeneous aerosols. *J. Appl. Meteorol. Climatol.* 56, 2141–2153. <https://doi.org/10.1175/JAMC-D-16-0320.1>.

Sherpherd, J.M., 2005. A review of current investigations of urban-induced rainfall and recommendations for the future. *Earth Interact.* 9, 1–27. <https://doi.org/10.1175/EI156.1>.

Sheridan, S.C., 2002. The redevelopment of a weather-type classification scheme for North America. *Int. J. Climatol.* 22, 51–68. <https://doi.org/10.1002/joc.709>.

Sheridan, S.C., Power, H.C., Senkbeil, J.C., 2008. A further analysis of the spatio-temporal variability in aerosols across North America: incorporation of lower tropospheric (850-hPa) flow. *Int. J. Climatol.* 28, 1189–1199. <https://doi.org/10.1002/joc.1628>.

Shi, Z., Wang, H., Tan, Y., Li, L., Li, C., 2020. Influence of aerosols on lightning activities in central eastern parts of China. *Atmos. Sci. Lett.* 21 <https://doi.org/10.1002/asl.957>.

Stallins, J.A., Carpenter, J., Bentley, M.L., Ashley, W.S., Mulholland, J.A., 2013. Weekend-weekday aerosols and geographic variability in cloud-to-ground lightning for the urban region of Atlanta, Georgia, USA. *Reg. Environ. Chang.* 13, 137–151. <https://doi.org/10.1007/s10113-012-0327-0>.

Stensrud, D.J., 1996. Importance of low-level jets to climate: a review. *J. Clim.* 9, 1698–1711. [https://doi.org/10.1175/1520-0442\(1996\)009<1698:ILLJT>2.0.CO;2](https://doi.org/10.1175/1520-0442(1996)009<1698:ILLJT>2.0.CO;2).

Stevens, B., Feingold, G., 2009. Untangling aerosol effects on clouds and precipitation in a buffered system. *Nature* 461, 607–613. <https://doi.org/10.1038/nature08281>.

Stoltz, D.C., Rutledge, S.A., Pierce, J.R., Heever, S.C., 2017. A global lightning parameterization based on statistical relationships among environmental factors, aerosols, and convective clouds in the TRMM climatology. *J. Geophys. Res. Atmos.* 122, 7461–7492. <https://doi.org/10.1002/2016JD026220>.

Storer, R.L., Van Den Heever, S.C., Stephens, G.L., 2010. Modeling aerosol impacts on convective storms in different environments. *J. Atmos. Sci.* 67, 3904–3915. <https://doi.org/10.1175/2010JAS3363.1>.

Storer, R.L., Van Den Heever, S.C., L'Ecuyer, T.S., 2014. Observations of aerosol-induced convective invigoration in the tropical East Atlantic. *J. Geophys. Res. Atmos.* 119, 3963–3975. <https://doi.org/10.1002/2013JD020272>.

Sun, M., Qie, X., Mansell, E.R., Liu, D., Yair, Y., Fierro, A.O., Yuan, S., Lu, J., 2023. Aerosol impacts on storm electrification and lightning discharges under different thermodynamic environments. *JGR-Atmos.* 128 <https://doi.org/10.1029/2022JD037450> e2022JD037450.

Tan, Y.B., Peng, L., Shi, Z., Chen, H.R., 2016. Lightning flash density in relation to aerosol over Nanjing (China). *Atmos. Res.* 174–175, 1–8. <https://doi.org/10.1016/j.atmos.2016.01.009>.

Tao, W.-K., Li, X., Khain, A., Matsui, T., Lang, S., Simpson, J., 2007. Role of atmospheric aerosol concentration on deep convective precipitation: Cloud-resolving model simulations. *J. Geophys. Res.* 112, D24S18. <https://doi.org/10.1029/2007JD008728>.

Tao, W.-K., Chen, J.-P., Li, Z., Wang, C., Zhang, C., 2012. Impact of aerosols on convective clouds and precipitation: aerosol impact on convective clouds. *Rev. Geophys.* 50 <https://doi.org/10.1029/2011RG000369>.

Tuomi, T.J., Larjavaara, M., 2005. Identification and analysis of flash cells in thunderstorms. *Q. J. R. Meteorol. Soc.* 131, 1191–1214. <https://doi.org/10.1256/qj.04.64>.

Tuttle, J.D., Davis, C.A., 2006. Corridors of warm season precipitation in the Central United States. *Mon. Weather Rev.* 134, 2297–2317. <https://doi.org/10.1175/MWR3188.1>.

United States Census Bureau, 2021. January 12.

van den Heever, S.C., Cotton, W.R., 2007. Urban aerosol impacts on downwind convective storms. *J. Appl. Meteorol. Climatol.* 46 (6), 828–850. <https://doi.org/10.1175/JAM2492.1>.

van den Heever, S.C., Carrión, G.G., Cotton, W.R., DeMott, P.J., Prenni, A.J., 2006. Impacts of nucleating aerosol on Florida storms. Part I: mesoscale simulations. *J. Atmos. Sci.* 63, 1752–1775. <https://doi.org/10.1175/JAS3713.1>.

van den Heever, S.C., Stephens, G.L., Wood, N.B., 2011. Aerosol indirect effects on tropical convection characteristics under conditions of radiative-convective equilibrium. *J. Atmos. Sci.* 68, 699–718. <https://doi.org/10.1175/2010JAS3603.1>.

Wall, C., Zipser, E., Liu, C., 2014. An investigation of the aerosol indirect effect on convective intensity using satellite observations. *J. Atmos. Sci.* 71, 430–447. <https://doi.org/10.1175/JAS-D-13-0158.1>.

Wang, S.-Y., Chen, T.-C., 2009. The late-spring maximum of rainfall over the U.S. Central Plains and the role of the low-level jet. *J. Clim.* 22, 4696–4709. <https://doi.org/10.1175/2009JCLI2719.1>.

Wang, J., van den Heever, S.C., Reid, J.S., 2009. A conceptual model for the link between central American biomass burning aerosols and severe weather over the south Central United States. *Environ. Res. Lett.* 4, 015003 <https://doi.org/10.1088/1748-9326/4/1/015003>.

Wang, Y., Wan, Q., Meng, W., Liao, F., Tan, H., Zhang, R., 2011. Long-term impacts of aerosols on precipitation and lightning over the Pearl River Delta megacity area in China. *Atmos. Chem. Phys.* 11, 12421–12436. <https://doi.org/10.5194/acp-11-12421-2011>.

Wang, Q., Li, Z., Guo, J., Zhao, C., Cribb, M., 2018. The climate impact of aerosols on the lightning flash rate: is it detectable from long-term measurements? *Atmos. Chem. Phys.* 18, 12797–12816. <https://doi.org/10.5194/acp-18-12797-2018>.

Wang, H., Tan, Y., Shi, Z., Yang, N., Zheng, T., 2023a. Diurnal differences in the effect of aerosols on cloud-to-ground lightning in the Sichuan Basin. *Atmos. Chem. Phys.* 23, 2843–2857. <https://doi.org/10.5194/acp-23-2843-2023>.

Wang, Y., Wang, Y., Song, X., Shang, Y., Zhou, Y., Huang, X., Zhanqing, L., 2023b. The impact of particulate pollution control on aerosol hygroscopicity and CCN activity in North China. *Environ. Res. Lett.* 18, 074028 <https://doi.org/10.1088/1748-9326/acde91>.

Williams, E., Stanfill, S., 2002. The physical origin of the land–ocean contrast in lightning activity. *C. R. Phys.* 3, 1277–1292. [https://doi.org/10.1016/S1631-0705\(02\)01407-X](https://doi.org/10.1016/S1631-0705(02)01407-X).

Williams, E., et al., 2002. Contrasting convective regimes over the Amazon: implications for cloud electrification. *J. Geophys. Res.* 107, 8082. <https://doi.org/10.1029/2001JD000380>.

Williams, E., Chan, T., Boccippio, D., 2004. Islands as miniature continents: Another look at the land–ocean lightning contrast. *J. Geophys. Res.* 109, D16206. <https://doi.org/10.1029/2003JD003833>.

Williams, E., Mushtak, V., Rosenfeld, D., Goodman, S., Boccippio, D., 2005. Thermodynamic conditions favorable to superlative thunderstorm updraft, mixed phase microphysics and lightning flash rate. *Atmos. Res.* 76, 288–306. <https://doi.org/10.1016/j.atmosres.2004.11.009>.

Wu, Z.J., Poulain, L., Henning, S., Dieckmann, K., Birnili, W., Merkel, M., van Pinxteren, D., Spindler, G., Müller, K., Stratmann, F., Herrmann, H., Wiedensohler, A., 2013. Relating particle hygroscopicity and CCN activity to chemical composition during the HCCT-2010 field campaign. *Atmos. Chem. Phys.* 13, 7983–7996. <https://doi.org/10.5194/acp-13-7983-2013>.

Yair, Y.Y., Lynn, B.H., Korzets, M., Jaffe, M., 2022. The “Weekend Effect” in lightning activity during winter thunderstorms over the Tel-Aviv, Israel, metropolitan area. *Atmosphere* 13, 1570. <https://doi.org/10.3390/atmos13101570>.

Zhang, Y., Tang, L., Croteau, P.L., Favez, O., Sun, Y., Canagaratna, M.R., Wang, Z., Couvidat, F., Albinet, A., Zhang, H., Sciare, J., Prévôt, A.S.H., Jayne, J.T., Worsnop, D.R., 2017. Field characterization of the PM_{2.5} Aerosol Chemical Speciation Monitor: insights into the composition, sources, and processes of fine particles in eastern China. *Atmos. Chem. Phys.* 17, 14501–14517. <https://doi.org/10.5194/acp-17-14501-2017>.

Zhong, S., Fast, J.D., Bian, X., 1996. A case study of the great plains low-level jet using wind profiler network data and a high-resolution mesoscale model. *Mon. Weather Rev.* 124, 785–806. [https://doi.org/10.1175/1520-0493\(1996\)124<0785:ACSOTG>2.0.CO;2](https://doi.org/10.1175/1520-0493(1996)124<0785:ACSOTG>2.0.CO;2).

Zhu, Y., Rosenfeld, D., Yu, X., Liu, G., Dai, J., Xu, X., 2014. Satellite retrieval of convective cloud base temperature based on the NPP/VIIRS Imager. *Geophys. Res. Lett.* 41 (4), 1308–1313. <https://doi.org/10.1002/2013GL058970>.

Zhu, Y., Rosenfeld, D., Yu, X., Li, Z., 2015. Separating aerosol microphysical effects and satellite measurement artifacts of the relationships between warm rain onset height and aerosol optical depth. *J. Geophys. Res. Atmos.* 120 (15), 7726–7736. <https://doi.org/10.1002/2015JD023547>.

Zipser, E.J., 2003. Some views on “Hot Towers” after 50 years of Tropical Field Programs and two years of TRMM Data. In: Tao, W.-K., Adler, R. (Eds.), *Cloud Systems, Hurricanes, and the Tropical Rainfall Measuring Mission (TRMM)*. American Meteorological Society, Boston, MA, pp. 49–58. https://doi.org/10.1007/978-1-878220-63-9_5.